



# Design of $L_2$ stable fixed-order decentralised controllers in a network of sampled-data systems with time-delays

Deesh Dileep, Jijju Thomas, Laurentiu Hetel, Nathan van De Wouw,  
Jean-Pierre Richard, Wim Michiels

## ► To cite this version:

Deesh Dileep, Jijju Thomas, Laurentiu Hetel, Nathan van De Wouw, Jean-Pierre Richard, et al..  
Design of  $L_2$  stable fixed-order decentralised controllers in a network of sampled-data systems with  
time-delays. European Journal of Control, 2020, 10.1016/j.ejcon.2020.02.002 . hal-02505298

**HAL Id: hal-02505298**

**<https://hal.science/hal-02505298>**

Submitted on 11 Mar 2020

**HAL** is a multi-disciplinary open access archive for the deposit and dissemination of scientific research documents, whether they are published or not. The documents may come from teaching and research institutions in France or abroad, or from public or private research centers.

L'archive ouverte pluridisciplinaire **HAL**, est destinée au dépôt et à la diffusion de documents scientifiques de niveau recherche, publiés ou non, émanant des établissements d'enseignement et de recherche français ou étrangers, des laboratoires publics ou privés.

# Design of $\mathcal{L}_2$ stable fixed-order decentralised controllers in a network of sampled-data systems with time-delays<sup>★</sup>

Deesh Dileep<sup>a,b,c,\*</sup>, Jijju Thomas<sup>b,c,d</sup>, Laurentiu Hetel<sup>b</sup>, Nathan van de Wouw<sup>d,e</sup>, Jean-Pierre Richard<sup>b,c</sup> and Wim Michiels<sup>a</sup>

<sup>a</sup>Department of Computer Science, KU Leuven, 3001 Leuven, Belgium

<sup>b</sup>University of Lille, UMR 9189 - CRISTAL, CNRS, Centrale Lille, France

<sup>c</sup>Inria, Lille, France

<sup>d</sup>Department of Mechanical Engineering, TU Eindhoven, 5600 MB Eindhoven, The Netherlands

<sup>e</sup>Department of Civil, Environmental and Geo-Engineering, University of Minnesota, Minneapolis, USA

## ARTICLE INFO

### Keywords:

decentralized control  
time-delay systems  
sampled-data control  
network structure exploitation  
robust controller design

## ABSTRACT


A methodology is proposed for the design of sampled-data fixed-order decentralised controllers for Multiple Input Multiple Output (MIMO) Linear Time-Invariant (LTI) time-delay systems. Imperfections in the communication links between continuous-time plants and controllers arising due to transmission time-delays, aperiodic sampling, and asynchronous sensors and actuators are considered. We model the errors induced due to the control imperfections using an operator approach leading to a simple  $\mathcal{L}_2$  stability criterion. A frequency domain-based direct optimisation approach towards controller design is proposed in this paper. This approach relies on the minimisation of cost functions, for stability and robustness against control imperfections, as a function of the controller or design parameters. First, the proposed method towards controller design is applied to generic MIMO LTI systems with time-delays. Second, when the delay system to be controlled has the structure of a network of coupled quasi-identical subsystems, we use a scalable algorithm to design identical decentralised controllers through network structure exploitation. Quasi-identical subsystems are identical subsystems that have non-identical uncertainties or control imperfections. By exploiting the structure, we improve the computational efficiency and scalability with the number of subsystems. The methodology has been implemented in a publicly available software, which supports system models in terms of delay differential algebraic equations. Finally, the effectiveness of the methodology is illustrated using a numerical example.

## 1. Introduction

For large-scale systems, decentralised controllers are generally preferred over centralised controllers due to their practicality and costs involved [28, 40]. However, designing decentralised controllers is challenging since they have to collectively meet global objectives while acting (and sensing) locally. Time-delays are present in many large-scale systems as the transfer of energy, material, or information is usually not instantaneous. Many applications such as power systems [29, 44] and automated vehicular platoons [45] could be modelled as interconnected time-delay systems. For these applications, stability and performance levels may be guaranteed for their (respective) continuous time system models. However, when implemented digitally, the information is not available in continuous time [21], the clocks at the sensors and actuators may not be operating synchronously [21, 26], and the individual sampling sequences may be aperiodic [3, 23, 46]. For real-world applications, we can also encounter situations where the local clocks at the sensor and at the actuator are not synchronized [12, 43]. In general, synchronization of clocks over networks induces fundamental limitations [14]. For power system applica-

tions, it has been shown in [22] that GPS synchronization may be vulnerable against malicious attacks. This motivates the study of decentralised sampled-data controllers. To the best of the authors' knowledge, this is largely an open problem. Some problem formulations in the literature are close to the problem considered in this paper. For example, the problem of how large the clock offset between actuator and sensor can be for the centralised control configuration, without compromising the existence of a stabilizing linear time-invariant controller was already addressed in [43]. Other problem formulations, related to the topic studied in this paper, include decentralised event triggered control [10] and decentralised observer-based feedback control for plants with networked communication (modelled as switched systems) [4]. In [10], sampling interval is considered to be a control parameter. In general, sampling intervals could be arbitrary and cannot be controlled, similar to the case considered in this paper. The stability analysis of LTI systems with distributed sensors and aperiodic sampling was dealt with in [13] and was extended to include static decentralised controllers and time-varying control computation delays in [41]. However, designing the decentralised sampled-data controllers for time-delay systems is largely an open problem.

In the literature, sampled-data systems are modelled as Time-Delay Systems (TDSs) [15, 34], hybrid systems [10, 37], discrete-time switched systems with varying pa-

 deesh.dileep@kuleuven.be (D. Dileep); jijju.thomas@inria.fr (J. Thomas); laurentiu.hetel@centralelille.fr (L. Hetel); N.v.d.Wouw@tue.nl (N.v.d. Wouw); jean-pierre.richard@ec-lille.fr (J. Richard); wim.michiels@cs.kuleuven.be (W. Michiels)  
ORCID(s): 0000-0003-1880-0746 (D. Dileep)

rameters [11], feedback interconnections of systems [16], etc. We refer to the recent survey paper of [20] for a general overview of the topic. In this paper, the case of Linear Time-Invariant (LTI) systems with time-delays (at state, controlled input, and measured output) of retarded type is addressed from a feedback interconnection point of view. We focus on both stability conditions and design approaches for sampled-data fixed-order decentralised controllers for LTI systems with constant delays. For generality, we take into account several imperfections in control implementation such as aperiodic sampling, time-delays, and asynchronous operation of controllers. Moreover, two types of time-delays are considered in this paper. First, constant time-delays which are present in the continuous-time system models. Second, time-varying delays in the communication network between plants and controllers.

The main contributions of this paper are three-fold. First, stability conditions are presented for generic LTI systems with constant time-delays (at input, output, and state) stabilised by fixed-order decentralised controllers taking into account control imperfections (induced by the implementation of the sampled-data controller with feedback delays). The approach is based on rewriting the closed-loop system of the Multiple Input Multiple Output (MIMO) plant and sampled-data fixed-order controllers as a feedback interconnection of a nominal (continuous time) Delay Differential Algebraic Equations (DDAEs) and an uncertainty block. Then, an input-output  $\mathcal{L}_2$  stability criterion is proposed. All the control imperfections are “absorbed” at the uncertainty (operator) block in this feedback interconnection [17, 24, 25].

As a second contribution, we propose to optimise the controller parameters for robustness against control imperfections by minimising the  $\mathcal{H}_\infty$  norm of an appropriately defined transfer function. Additionally, it is shown that the conservatism of the optimised robustness criterion can be reduced by exploiting the structure of the uncertainty block using “scaling” parameters. The methodology used to design these parameters is grounded in the frequency domain-based direct optimisation approach of [9, 18, 32], where objective functions specifying performance criteria are optimised as a function of the controller parameters. The adopted frequency domain-based optimisation approach for controller parameters complements the approach for infinite dimensional systems considered in [2]. This approach is flexible in exploiting the structure of the controller. Structures such as decentralised, distributed, overlapping, lower-order, and PID<sup>1</sup> controllers can be handled.

As a third contribution and main result of this paper, a scalable controller design approach is proposed for large-scale systems composed of quasi-identical subsystems connected through some delayed network. This case is inspired from real-world applications of multi-agent systems and consensus or synchronization problems, for example, an automated vehicular platoon may be considered as a group of

quasi-identical systems which are communicating through a network [9, 45]. Moreover, many researchers acknowledge the need to develop scalable and computationally efficient algorithms for control that have the following features: distributed and deployable at large scales, supported by local decisions and global coordination, and robust against asynchronous operation and inconsistent information [26]. In applications such as power systems [44] and automated vehicular platoons [45], controllers are often implemented as algorithms programmed on embedded processors manufactured by different companies which might work at different temporal frequencies. In this paper, identical subsystems that have non-identical uncertainties or control imperfections are considered to be quasi-identical subsystems. The control design problem is solved for a lower-dimensional system using network structure exploitation (see [9]) while guaranteeing stability of the large network.

The remainder of the paper is organised as follows. Section 2 introduces the MIMO time-delay plants which are to be stabilised by sampled-data decentralised controllers. Section 3 recasts the problem of maximizing robustness against the control imperfections to a standard  $\mathcal{H}_\infty$  norm optimisation problem. Section 4 presents the direct optimisation approach in the frequency domain to optimise robustness (in terms of  $\mathcal{H}_\infty$  norm) of the controllers against control imperfections. This  $\mathcal{H}_\infty$  norm characterises the maximum allowable uncertainty. Section 4.2 recalls the concept of network structure exploitation and how it may be utilised to improve computational efficiency in designing decentralised controllers that are robust (against control imperfections). A numerical example is presented in Section 5. Finally, some concluding remarks are given in Section 6.

We use the following notations throughout the paper.  $\mathbb{N}$  is the set of all natural numbers.  $\mathbb{R}$  is the set of all real numbers.  $\mathbb{R}^n$  is the  $n$ -dimensional real vector space.  $\mathbb{Z}$ ,  $\mathbb{Z}_0^+$ , and  $\mathbb{Z}^-$  are the sets of all integers, non-negative integers, and negative integers, respectively. The Kronecker product is denoted by  $\otimes$ .  $\Re(\lambda)$  is the real part of complex number  $\lambda$ .  $\sigma_1(G)$  is the maximum singular value of matrix  $G$ .  $\mathcal{L}_{2e}(a, b)$  is the extended  $\mathcal{L}_2$ -space of all square integrable and Lebesgue measurable functions defined on the interval  $(a, b)$  of appropriate dimension.

## 2. MIMO plant and decentralised controllers

In many applications, communication of sensor data and actuation commands are distributed over different communication channels which may function aperiodically and asynchronously. In this paper, we first consider a generic Multiple Input Multiple Output (MIMO) continuous time plant with  $N \in \mathbb{N}$  inputs and outputs, to be controlled by  $N$  decentralised dynamic controllers. The dynamics of the Linear Time Invariant (LTI) MIMO plants with constant time-

<sup>1</sup>See the recent survey of [38], wherein PID controllers still have a strong industrial impact.

delays considered in this paper are described by

$$\begin{cases} \dot{\psi}_p(t) &= A_{\psi_p,0} \psi_p(t) + \sum_{j=1}^m A_{\psi_p,j} \psi_p(t - \tau_{\psi,j}) \\ &+ \sum_{i=1}^N B_{\psi_p,i} u_i(t - \tau_{u,i}), \\ y_i(t) &= C_{\psi_p,i} \psi_p(t - \tau_{y,i}), \quad i = 1, \dots, N, \end{cases} \quad (1)$$

for almost all  $t \geq 0$ , where  $\dot{\psi}_p$  is the right-hand derivative of the (instantaneous) state vector  $\psi_p$ ,  $u_i \in \mathbb{R}^{n_{u,i}}$  is the  $i^{\text{th}}$  controlled-input,  $y_i \in \mathbb{R}^{n_{y,i}}$  is the  $i^{\text{th}}$  measured-output,  $\psi_p \in \mathbb{R}^{n_p}$  is the plant state vector,  $\tau_{\psi,j}, \tau_{y,i}, \tau_{u,i} > 0$  are constant delays, and  $A_{\psi_p,0}, A_{\psi_p,j}, C_{\psi_p,i}, B_{\psi_p,i}$  are real valued constant matrices,  $i = 1, \dots, N, j = 1, \dots, m$ . It has been shown in [8, 9, 32] that plants of the form (1) can be rewritten in the general DDAE form with time-delays present only at the state. Plants of the form (1) can be rewritten in the DDAE form as

$$\begin{cases} E_p \dot{x}_p(t) &= A_{p0} x_p(t) + \sum_{j=1}^{m_n} A_{pj} x_p(t - \tau_j) \\ &+ \sum_{i=1}^N B_{pi} u_i(t), \\ y_i(t) &= C_{pi} x_p(t), \quad i = 1, \dots, N, \end{cases} \quad (2)$$

where  $x_p = [\psi_p^T \gamma_{\psi,y}^T \gamma_{\psi,u}^T]^T$  is the augmented (instantaneous) state vector,  $\gamma_{\psi,y}$  and  $\gamma_{\psi,u}$  are dummy vectors used for representing output vector  $y = [y_1^T, \dots, y_N^T]^T$  and input vector  $u = [u_1^T, \dots, u_N^T]^T$  respectively, and  $E_p$  may be singular. Notice that all the time-delays are now associated with the augmented state vector, that is,  $\{\tau_1, \dots, \tau_{m_n}\} = \{\tau_{\psi,1}, \dots, \tau_{\psi,m}\} \cup \{\tau_{y,1}, \dots, \tau_{y,N}\} \cup \{\tau_{u,1}, \dots, \tau_{u,N}\}$ . Then,  $m$  is the number of distinct time-delays present at the state and  $m_n$  is the number of distinct time-delays present at the state, inputs, and outputs ( $m_n \geq m$ ). Sections 2.1-2.2 will introduce sampled-data controllers for plants of form (2) and a related input-output  $\mathcal{L}_2$  stability criterion.

Furthermore, a particular class of systems of form (2) is also considered, for which the computational efficiency of the controller design algorithm can be improved. The particular class of systems consists of “ $N$ ” identical subsystems coupled through a network graph. We consider a network described by a directed graph  $\mathcal{G} = \{\mathcal{V}, \mathcal{E}, A_M\}$  with a set of nodes  $\mathcal{V} = \{1, 2, \dots, N\}$  and a set of edges  $\mathcal{E} \subset \mathcal{V} \times \mathcal{V}$ . The edge  $(i, j) \in \mathcal{E}$  connects from node  $j \in \mathcal{V}$  to node  $i \in \mathcal{V}$ .  $A_M$  is the adjacency matrix of the corresponding network structure, with  $a_{M,i,j} \geq 0$  being the entry at row  $i$  and column  $j$ . The adjacency matrix is a square matrix with zero diagonal elements and its off-diagonal element ( $a_{M,i,j}$ ) is considered to be the weight of the corresponding edge  $(i, j)$ . The graph  $\mathcal{G}$  does not need to be strongly connected. We assume that the associated time-delays and the information exchange between these subsystems are identical. Then, the particular class of MIMO systems of form (1) can be rewritten as

$$\begin{cases} \dot{\psi}_{pi}(t) &= \bar{A}_{\psi_p,0} \psi_{pi}(t) + \sum_{j=1}^m \bar{A}_{\psi_p,j} \psi_{pi}(t - \tau_{\psi,j}) \\ &+ \bar{B}_{\psi_p} u_i(t - \tau_u) + \bar{B}_{uc} u_{ci}(t - \tau_{uc}), \\ y_i(t) &= \bar{C}_{\psi_p} \psi_{pi}(t - \tau_y), \quad i = 1, \dots, N, \end{cases} \quad (3)$$

which corresponds to the nodal dynamics and their intercon-

nection is described by the coupling term

$$u_{ci}(t) = \sum_{j=1, j \neq i}^N a_{M,i,j} \psi_{pj}(t), \quad (4)$$

where  $\dot{\psi}_{pi}$  is the right-hand derivative of the state vector  $\psi_{pi}$  corresponding to subsystem  $i$ ,  $\tau_{uc} > 0$ ,  $\tau_y > 0$ ,  $\tau_u > 0$  are constant delays, and  $\bar{A}_{\psi_p,0}, \bar{A}_{\psi_p,j}, \bar{C}_{\psi_p}, \bar{B}_{\psi_p}, \bar{B}_{uc}$  are real valued constant matrices,  $i = 1, \dots, N$ . Similar to generic plants of form (1), plants of form (3)-(4) can also be re-written in the DDAE form as

$$\begin{cases} \bar{E}_p \dot{x}_{pi}(t) &= \bar{A}_{p0} x_{pi}(t) + \sum_{j=1, j \neq i}^N a_{M,i,j} \bar{F}_p x_{pj}(t) \\ &+ \sum_{k=1}^{m_n} \bar{A}_{pk} x_{pi}(t - \tau_k) + \bar{B}_p u_i(t), \\ y_i(t) &= \bar{C}_p x_{pi}(t), \quad i = 1, \dots, N. \end{cases} \quad (5)$$

The above system model is also in the most general DDAE form since  $\bar{E}_p$  is allowed to be singular. Hence, this system can also be used to represent subsystems which are delay coupled with the help of an augmented state vector [9]. The design of robust (identical) decentralised controllers for such systems can be made computationally efficient using the network structure exploitation approach developed in [9]. The corresponding approach will be discussed in Section 4.2.

In this paper, we focus on the (non-identical) control imperfections induced by aperiodic and asynchronous sample and hold functions at the interconnections between sensors, decentralised controllers, and actuators. However, as we shall illustrate with an example in Section 5, the adopted approach based on the small gain theorem trivially extends to combining other ( $\mathcal{L}_2$ -bounded) uncertainties such as parametric uncertainties. That is, for the particular case where (sub-)systems are coupled in a network, the assumption of identical subsystems can be relaxed (only the nominal subsystem models need to be identical) [27]. In the following subsection, we define the decentralised sampled-data controllers used to stabilize systems of form (1).

## 2.1. Sampled-data decentralised control

The sampling and actuation sequences for control are introduced in this section. An overview of the sampled-data control configuration is shown in Figure 1 and the corresponding symbols are defined as follows. The  $i^{\text{th}}$  measured output ( $y_i(t)$ ) is sampled according to a sampling sequence  $\{s_k^i\}_{k \in \mathbb{Z}_0^+}$ , represented using a set of instants, where  $s_0^i \in (0, \bar{h}_i]$ ,

$$s_{k+1}^i = s_k^i + h_k^i, \quad (6)$$

and  $h_k^i \in (0, \bar{h}_i]$ ,  $k \in \mathbb{Z}_0^+$ ,  $i = 1, \dots, N$ . The sampling intervals ( $h_k^i$ ) consider imperfections in sampling such as jitters and data packet dropouts. The sequence of instants at which the  $i^{\text{th}}$  controller receives the sampled output is denoted by  $\{\rho_k^i\}_{k \in \mathbb{Z}_0^+}$ , where

$$\rho_k^i = s_k^i + \vartheta_k^i, \quad (7)$$

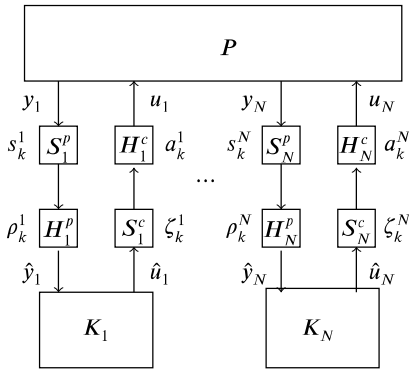


**Figure 1:** The closed-loop system of the decentralised controllers ( $K_i$ ) and the MIMO plant ( $P$ ) with constant time-delays and control imperfections.  $S_i^p - H_i^p$  and  $S_i^c - H_i^c$  represent the sample and hold functions from the  $i^{\text{th}}$  sensor to the  $i^{\text{th}}$  controller and from the  $i^{\text{th}}$  controller to the  $i^{\text{th}}$  actuator, respectively,  $i = 1, \dots, n$ .  $\{s_k^i\}_{k \in \mathbb{Z}_0^+}$ ,  $\{\rho_k^i\}_{k \in \mathbb{Z}_0^+}$ ,  $\{\zeta_k^i\}_{k \in \mathbb{Z}_0^+}$ , and  $\{a_k^i\}_{k \in \mathbb{Z}_0^+}$  are the corresponding sequences in time when the sample and hold functions are implemented.

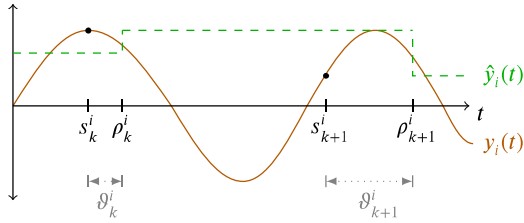


**Figure 2:** A random output signal ( $y_i(t)$ ) is sampled according to a sampling sequence  $\{s_k^i\}_{k \in \mathbb{Z}_0^+}$ ,  $i = 1, \dots, N$ . The signal available at the  $i^{\text{th}}$  controller ( $\hat{y}_i(t)$ ) is an implementation of the sampled output ( $y_i(s_k^i)$ ) at an interval  $[\rho_k^i, \rho_{k+1}^i)$ ,  $k \in \mathbb{Z}_0^+$ ,  $i = 1, \dots, N$ .

and  $\vartheta_k^i \in [0, \bar{\vartheta}_i]$ ,  $k \in \mathbb{Z}_0^+$ ,  $i = 1, \dots, N$ . The asynchrony between sensors and controllers are denoted by  $\vartheta_k^i$ ,  $k \in \mathbb{Z}_0^+$ ,  $i = 1, \dots, N$ . We consider the sampled-output received at the controller to be

$$\hat{y}_i(t) = \begin{cases} y_i(0), & \forall t \in [0, \rho_0^i), \\ y_i(s_k^i), & \forall t \in [\rho_k^i, \rho_{k+1}^i), \end{cases} \quad (8)$$

for all  $k \in \mathbb{Z}_0^+$ ,  $i = 1, \dots, N$ , see Figure 2. We consider the dynamics of the  $i^{\text{th}}$  fixed-order controller to be

$$\begin{aligned} \dot{x}_{ci}(t) &= A_{ci} x_{ci}(t) + B_{ci} \hat{y}_i(t), \\ \hat{u}_i(t) &= C_{ci} x_{ci}(t) + D_{ci} \hat{y}_i(t), \end{aligned} \quad (9)$$

for almost all  $t \geq 0$ , where the controller state is denoted by  $x_{ci}(t) \in \mathbb{R}^{n_{ci}}$ , the controller coefficient matrices  $A_{ci}$ ,  $B_{ci}$ ,  $C_{ci}$ , and  $D_{ci}$  are constant and real valued. The  $i^{\text{th}}$  input computed by the controller ( $\hat{u}_i(t)$ ) is sampled according to a sequence  $\{\zeta_k^i\}_{k \in \mathbb{Z}_0^+}$  where  $\zeta_0^i \in (0, \bar{\kappa}_i]$ ,

$$\zeta_{k+1}^i = \zeta_k^i + \kappa_k^i, \quad (10)$$

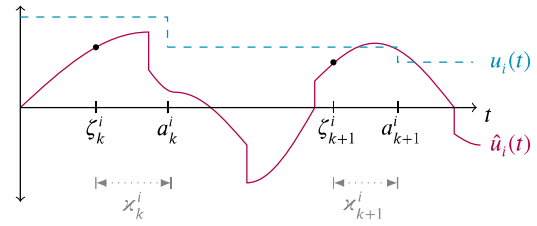


**Figure 3:** A random input signal ( $\hat{u}_i(t)$ ) computed at the  $i^{\text{th}}$  controller is sampled according to a sampling sequence  $\{\zeta_k^i\}_{k \in \mathbb{Z}_0^+}$ ,  $i = 1, \dots, N$ . The signal available at the  $i^{\text{th}}$  actuator ( $u_i(t)$ ) is an implementation of the sampled input ( $\hat{u}_i(\zeta_k^i)$ ) at an interval  $[a_k^i, a_{k+1}^i)$ ,  $k \in \mathbb{Z}_0^+$ ,  $i = 1, \dots, N$ . The generated input signal ( $\hat{u}_i(t)$ ) is the sum of the continuous-time signal corresponding to the state of the controller ( $C_{ci}x_{ci}(t)$ ) and the piecewise continuous signal corresponding to the sampled output received at the controller ( $D_{ci}\hat{y}_i(t)$ ).

and  $\kappa_k^i \in (0, \bar{\kappa}_i]$ ,  $k \in \mathbb{Z}_0^+$ ,  $i = 1, \dots, N$ . Asynchrony may occur when there are time-delays in the feedback or when controller update instants are different from the sampling instants of the measurements. The controlled-input is implemented at the plant according to actuation instants  $\{a_k^i\}_{k \in \mathbb{Z}_0^+}$ , where

$$a_k^i = \zeta_k^i + \kappa_k^i, \quad (11)$$

and  $\kappa_k^i \in [0, \bar{\kappa}_i]$ ,  $k \in \mathbb{Z}_0^+$ ,  $i = 1, \dots, N$ . Here,  $\kappa_k^i$  denote the asynchrony between controllers and actuators (which includes computation delays in the controllers). The controlled-input implemented at the plant is

$$u_i(t) = \begin{cases} \hat{u}_i(0), & \forall t \in [0, a_0^i), \\ \hat{u}_i(\zeta_k^i), & \forall t \in [a_k^i, a_{k+1}^i), \end{cases} \quad (12)$$

for all  $k \in \mathbb{Z}_0^+$ ,  $i = 1, \dots, N$ , see Figure 3. Now, we consider the following assumption corresponding to the ordering of sampling and receiving instants of the closed-loop system (with control imperfections).

**Assumption 1.** We assume that the  $k^{\text{th}}$  closed-loop control sequence satisfies

$$0 < s_k^i \leq \rho_k^i \leq \zeta_k^i \leq a_k^i, \quad \forall k \in \mathbb{Z}_0^+, i = 1, \dots, N. \quad (13)$$

The above assumption (similar to that considered in [19, 35]) ensures that the output sampled at the instant  $s_k^i$  from the sensor is used for the computation of controlled-input at the instant  $\zeta_k^i$  which is implemented at the instant  $a_k^i$ . That is, the actuation data and control data are ordered with respect to the moments of time when sensor data is transmitted. This ensures that the control input based on  $y_i(s_k^i)$  can be applied at time-interval  $[a_k^i, a_{k+1}^i)$ ,  $k \in \mathbb{Z}_0^+$ . Notice that the contrary case  $\rho_k^i > \zeta_k^i$  would violate the causality principle where the  $k^{\text{th}}$  sequence input to the controller is received before the  $k^{\text{th}}$  sequence controlled input is computed. Also, the cases  $\rho_k^i > a_k^i$  or  $\zeta_k^i > a_k^i$  correspond to the cases where the  $k^{\text{th}}$  sequence



control data is processed before the  $k^{\text{th}}$  sequence actuation data is applied. Then, the asynchrony between sensors and actuators can be described by  $\{\eta_k^i\}_{k \in \mathbb{Z}_0^+}$ , where

$$\eta_k^i = a_k^i - s_k^i, \quad (14)$$

and  $\eta_k^i \in [0, \bar{\eta}_i]$ ,  $k \in \mathbb{Z}_0^+$ ,  $i = 1, \dots, N$ . We recall from Assumption 1 that  $x_{ci}(\zeta_k)$  and  $y_i(s_k)$  are the  $i^{\text{th}}$  controller state information and the measured-output from  $i^{\text{th}}$  plant, respectively, used for computing  $\hat{u}_i(\zeta_k^i)$ . Under Assumption 1, we have

$$\begin{aligned} \hat{u}_i(0) &= C_{ci}x_{ci}(0) + D_{ci}\hat{y}_i(0) = C_{ci}x_{ci}(0) + D_{ci}y_i(0), \\ \hat{u}_i(\zeta_k^i) &= C_{ci}x_{ci}(\zeta_k^i) + D_{ci}\hat{y}_i(\zeta_k^i) \\ &= C_{ci}x_{ci}(\zeta_k^i) + D_{ci}y_i(s_k^i), \end{aligned} \quad (15)$$

$k \in \mathbb{Z}_0^+$ ,  $i = 1, \dots, N$ .

**Remark 1.** The dynamics of PID controller may be represented in the frequency domain using the transfer function matrix

$$K_{PID}(s) = K_P + \frac{K_I}{s} + \frac{sK_D}{1 + \tau_d s},$$

where  $K_P$ ,  $K_I$ ,  $K_D$  are real valued gain matrices,  $s$  is the Laplace variable, and  $\tau_d$  is the time constant of the filter applied to the derivative action [30, 42]. Hence, it is also possible to represent decentralised PID controllers as (9) with some structure and tune their matrix gains for robustness against control imperfections using the approach proposed in this paper, see [8] for more details.

## 2.2. A feedback interconnection interpretation

In this subsection, we rewrite the closed-loop system of (2), (8), (9) and (12) as a feedback interconnection of a nominal system and an uncertainty block. This allows us to use a simple input-output  $\mathcal{L}_2$  stability criterion, extending the work of [13, 41] for dynamic controllers for DDAEs. For this purpose, we represent the piecewise-constant controlled-input and measured-output in continuous-time using time-varying errors, that is,

$$\begin{cases} \dot{x}_{ci}(t) &= A_{ci}x_{ci}(t) + B_{ci}(y_i(t) + e_1^i(t)), \\ u_i(t) &= (C_{ci}x_{ci}(t) + e_2^i(t)) + D_{ci}(y_i(t) + e_3^i(t)), \end{cases} \quad (16)$$

for all  $t \geq 0$ ,  $i = 1, \dots, N$ , where the error signals are

$$e_1^i(t) = \begin{cases} y_i(0) - y_i(t), & \forall t \in [0, \rho_0^i), \\ y_i(s_k^i) - y_i(t), & \forall t \in [\rho_k^i, \rho_{k+1}^i), \end{cases} \quad (17)$$

$$e_2^i(t) = \begin{cases} C_{ci}x_{ci}(0) - C_{ci}x_{ci}(t), & \forall t \in [0, a_0^i), \\ C_{ci}x_{ci}(\zeta_k^i) - C_{ci}x_{ci}(t), & \forall t \in [a_k^i, a_{k+1}^i), \end{cases} \quad (18)$$

$$e_3^i(t) = \begin{cases} y_i(0) - y_i(t), & \forall t \in [0, a_0^i), \\ y_i(s_k^i) - y_i(t), & \forall t \in [a_k^i, a_{k+1}^i), \end{cases} \quad (19)$$

for all  $k \in \mathbb{Z}_0^+$ ,  $i = 1, \dots, N$ . Here,  $e_1^i(t)$  arises due to the sampled output implemented at the controller,  $e_2^i(t)$  arises

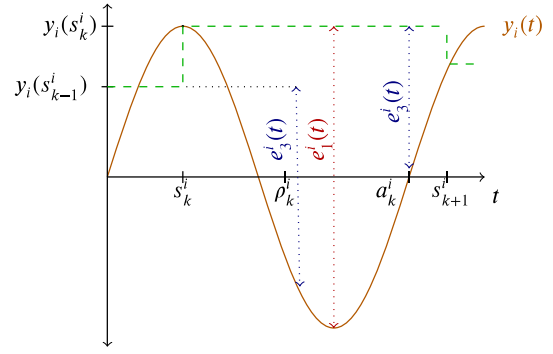


**Figure 4:** A signal  $y_i(t)$  used to illustrate that the errors  $e_1^i$  and  $e_3^i$  due to sampling need not be same.

due to the sampled controller-state implemented at the input, and  $e_3^i(t)$  arises due to the sampled output implemented at the input. Notice that  $e_1^i$  and  $e_3^i$  need not be same due to the transport delay, this is evident in Figure 4. Now we define the uncertainty operator. For this purpose, consider  $z_i = [z_{i,1}^T \ z_{i,2}^T]^T$ ,  $z_i \in \mathcal{L}_{2e}[0, \infty)$ ,  $w_i = [e_1^i \ e_3^i \ e_2^i]^T$ ,  $w_i \in \mathcal{L}_{2e}[0, \infty)$ , and the (bounded) integral operators  $\Delta_1^i$ ,  $\Delta_2^i$  and  $\Delta_3^i$  on  $\mathcal{L}_{2e}[0, \infty)$ ,  $i = 1, \dots, N$ , such that

$$\begin{aligned} e_1^i(t) &= (\Delta_1^i z_{i,1})(t) \\ &:= \begin{cases} -\int_0^t z_{i,1}(\theta) d\theta, & \forall t \in [0, \rho_0^i), \\ -\int_{s_k^i}^t z_{i,1}(\theta) d\theta, & \forall t \in [\rho_k^i, \rho_{k+1}^i), \end{cases} \end{aligned} \quad (20)$$

$$\begin{aligned} e_2^i(t) &= (\Delta_2^i z_{i,2})(t) \\ &:= \begin{cases} -\int_0^t z_{i,2}(\theta) d\theta, & \forall t \in [0, a_0^i), \\ -\int_{\zeta_k^i}^t z_{i,2}(\theta) d\theta, & \forall t \in [a_k^i, a_{k+1}^i), \end{cases} \end{aligned} \quad (21)$$

$$\begin{aligned} e_3^i(t) &= (\Delta_3^i z_{i,1})(t) \\ &:= \begin{cases} -\int_0^t z_{i,1}(\theta) d\theta, & \forall t \in [0, a_0^i), \\ -\int_{s_k^i}^t z_{i,1}(\theta) d\theta, & \forall t \in [a_k^i, a_{k+1}^i), \end{cases} \end{aligned} \quad (22)$$

for all  $k \in \mathbb{Z}_0^+$ ,  $i = 1, \dots, N$ . Let  $\tilde{\Delta}_i$  be an (uncertainty) operator on  $\mathcal{L}_{2e}[0, \infty)$  defined by

$$w_i(t) = (\tilde{\Delta}_i z_i)(t) := \begin{bmatrix} (\Delta_1^i z_{i,1})(t) \\ (\Delta_3^i z_{i,1})(t) \\ (\Delta_2^i z_{i,2})(t) \end{bmatrix}, \quad i = 1, \dots, N, \quad (23)$$

where  $w_i(t)$  is an exogenous input to the nominal system and  $z_i(t)$  is an exogenous output from the nominal system. We introduce the following proposition to recast the closed-loop system as a feedback interconnection of a continuous-time nominal system and an uncertainty block.

**Proposition 2.1.** Closed-loop system (2), (8), (9) and (12) can be rewritten as a feedback interconnection of a nominal system in the DDAE form (see Figure 5), using an augmented state vector  $x \in \mathbb{R}^{n_{cl}}$ ,

$$\begin{cases} E\dot{x}(t) = A_0x(t) + \sum_{j=1}^{m_n} A_jx(t - \tau_j) + Bw(t), \\ z(t) = Cx(t), \end{cases} \quad (24)$$

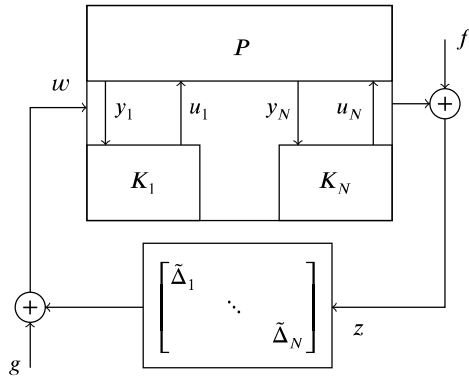


**Figure 5:** The control imperfections in Figure 1 are “absorbed” in the operators  $\tilde{\Delta}_i$ ,  $i = 1, \dots, N$ .

and an uncertainty operator on  $\mathcal{L}_{2e}[0, \infty)$  defined by

$$w(t) = (\tilde{\Delta}z)(t) := \begin{bmatrix} (\tilde{\Delta}_1 z_1)(t) \\ \vdots \\ (\tilde{\Delta}_N z_N)(t) \end{bmatrix}, \quad (25)$$

where  $w = [w_1^T \dots w_N^T]^T$ ,  $z = [z_1^T \dots z_N^T]^T$ , and  $E$ ,  $A_i$ ,  $B$ ,  $C$ ,  $i = 1, \dots, n$ , are real-valued coefficient matrices. Here,  $E$  is allowed to be a singular matrix.

**Proof.** Since the controlled-inputs are piecewise constant and there is no feed-through, the outputs  $y_i, i = 1, \dots, N$ , are piecewise continuously differentiable. That is, for any  $t_2 > t_1 \geq 0$ , we can express  $y_i(t_2) - y_i(t_1) = \int_{t_1}^{t_2} \dot{y}_i(\theta) d\theta \forall i = 1, \dots, N$ . Similarly, the functions  $C_{ci}x_{ci}, i = 1, \dots, N$ , are also piecewise continuously differentiable, then we can express  $C_{ci}x_{ci}(t_2) - C_{ci}x_{ci}(t_1) = \int_{t_1}^{t_2} C_{ci}\dot{x}_{ci}(\theta) d\theta, i = 1, \dots, N$ . Therefore, the errors can be rewritten as

$$\begin{aligned} e_1^i(t) &= \begin{cases} -\int_0^t \dot{y}_i(\theta) d\theta, & \forall t \in [0, \rho_0^i), \\ -\int_{s_k^i}^t \dot{y}_i(\theta) d\theta, & \forall t \in [\rho_k^i, \rho_{k+1}^i), \end{cases} \\ e_2^i(t) &= \begin{cases} -\int_0^t C_{ci}\dot{x}_{ci}(\theta) d\theta, & \forall t \in [0, a_0^i), \\ -\int_{a_k^i}^t C_{ci}\dot{x}_{ci}(\theta) d\theta, & \forall t \in [a_k^i, a_{k+1}^i), \end{cases} \\ e_3^i(t) &= \begin{cases} -\int_0^t \dot{y}_i(\theta) d\theta, & \forall t \in [0, a_0^i), \\ -\int_{s_k^i}^t \dot{y}_i(\theta) d\theta, & \forall t \in [a_k^i, a_{k+1}^i), \end{cases} \end{aligned} \quad (26)$$

for all  $k \in \mathbb{Z}_0^+$ ,  $i = 1, \dots, N$ . Then closed-loop system (2) and (16) can be rewritten in the feedback interconnection form of

$$\begin{cases} E_p \dot{x}_p(t) &= A_{p0} x_p(t) + \sum_{j=1}^{m_n} A_{pj} x_p(t - \tau_j) \\ &\quad + \sum_{i=1}^N B_{pi} u_i(t), \\ y_i(t) &= C_{pi} x_p(t), \\ \dot{x}_{ci}(t) &= A_{ci} x_{ci}(t) + B_{ci} y_i(t) + \begin{bmatrix} B_{ci} & 0 & 0 \end{bmatrix} w_i(t), \\ u_i(t) &= C_{ci} x_{ci}(t) + D_{ci} y_i(t) + \begin{bmatrix} 0 & I & D_{ci} \end{bmatrix} w_i(t), \\ z_i(t) &= \begin{bmatrix} \dot{y}_i(t) \\ C_{ci} \dot{x}_{ci}(t) \end{bmatrix}, \quad i = 1, \dots, N, \end{cases}$$

and

$$w_i(t) = (\tilde{\Delta}_i z_i)(t), \quad i = 1, \dots, N. \quad (28)$$

The plant in (24) is another simplified DDAE form of (27) where  $z_{i,1}(t) = \dot{y}_i(t)$ ,  $z_{i,2}(t) = C_{ci}\dot{x}_{ci}(t)$ ,  $i = 1, \dots, N$ , and the coefficient matrices in (24) are given by

$$A_0 = \begin{bmatrix} A_{p0} & B_p & 0 & 0 & 0 & 0 \\ 0 & -I & B_{w1} & 0 & C_c & D_c \\ 0 & 0 & -I & 0 & 0 & 0 \\ 0 & 0 & 0 & I & 0 & 0 \\ 0 & 0 & B_{w2} & 0 & A_c & B_c \\ C_p & 0 & 0 & 0 & 0 & -I \end{bmatrix},$$

$$A_i = \begin{bmatrix} A_{pi} & 0 & 0 & 0 & 0 & 0 \\ 0 & 0 & 0 & 0 & 0 & 0 \\ 0 & 0 & 0 & 0 & 0 & 0 \\ 0 & 0 & 0 & 0 & 0 & 0 \\ 0 & 0 & 0 & 0 & 0 & 0 \\ 0 & 0 & 0 & 0 & 0 & 0 \end{bmatrix},$$

$$C = \begin{bmatrix} 0 & 0 & 0 & I & 0 & 0 \end{bmatrix},$$

$$B = \begin{bmatrix} 0 & 0 & I & 0 & 0 & 0 \end{bmatrix}^T,$$

$$B_p = [B_{p1} \quad \dots \quad B_{pN}], \quad C_p = \begin{bmatrix} C_{p1} \\ \vdots \\ C_{pN} \end{bmatrix},$$

$$E = \begin{bmatrix} E_p & 0 & 0 & 0 & 0 & 0 \\ 0 & 0 & 0 & 0 & 0 & 0 \\ 0 & 0 & 0 & 0 & 0 & 0 \\ C_{z1} & 0 & 0 & 0 & C_{z2} & 0 \\ 0 & 0 & 0 & 0 & I & 0 \\ 0 & 0 & 0 & 0 & 0 & 0 \end{bmatrix},$$

$$C_c = \begin{bmatrix} C_{c1} & & 0 \\ & \ddots & \\ 0 & & C_{cN} \end{bmatrix}, \quad D_c = \begin{bmatrix} D_{c1} & & 0 \\ & \ddots & \\ 0 & & D_{cN} \end{bmatrix},$$

$$A_c = \begin{bmatrix} A_{c1} & & 0 \\ & \ddots & \\ 0 & & A_{cN} \end{bmatrix}, \quad B_c = \begin{bmatrix} B_{c1} & & 0 \\ & \ddots & \\ 0 & & B_{cN} \end{bmatrix},$$

$$B_{w1} = \begin{bmatrix} 0 & I & D_{c1} & & 0 \\ & & & \ddots & \\ 0 & & & & 0 & I & D_{cN} \end{bmatrix},$$

$$B_{w2} = \begin{bmatrix} B_{c1} & 0 & 0 & & 0 \\ & & & \ddots & \\ 0 & & & & B_{cN} & 0 & 0 \end{bmatrix},$$

$$C_{z1} = \begin{bmatrix} C_{p1} \\ 0 \\ \vdots \\ C_{pN} \\ 0 \end{bmatrix}, \quad C_{z2} = \begin{bmatrix} 0 & & 0 \\ C_{c1} & & \\ & \ddots & \\ 0 & & C_{cN} \end{bmatrix}.$$

The proof is complete.  $\circ$

**Remark 2.** Plant (24) is obtained by using the augmented state vector  $x = [x_p^T u^T \gamma_w^T \gamma_z^T x_c^T y^T]^T$ , where  $\gamma_w$  and  $\gamma_z$  are dummy vectors for  $w$  and  $z$ , respectively,  $x_c = [x_{c1}^T \dots x_{cN}^T]^T$ ,  $u = [u_1^T \dots u_N^T]^T$ , and  $y = [y_1^T \dots y_N^T]^T$ .

**Remark 3.** Plant (2) has no exogenous inputs or outputs. However, it is possible to consider other exogenous inputs (which will arise in the first line of (27)) or outputs in its dynamics in addition to the control imperfections. Such a system can also be recast into the form of (24) with minor changes in the coefficient matrices, input vector, and output vector.

Notice that by rewriting the system in the DDAE form (24), we have enforced all the controller parameters to be contained within  $A_0$ .

### 3. Stability criterion: generic case

Using the problem described in the previous section as our motivation, we study the feedback interconnection of a plant  $\mathbf{G}$  and an uncertainty block  $\tilde{\Delta}$

$$\begin{cases} z &= \mathbf{G}w + f, \\ w &= \tilde{\Delta}z + g, \end{cases} \quad (29)$$

where  $f, g \in \mathcal{L}_{2e}[0, \infty)$ . The operator  $\mathbf{G}$  on  $\mathcal{L}_{2e}[0, \infty)$  describes the input-output map of system (24). In the frequency domain, it is described by the transfer function matrix

$$G(s) := C(sE - A_0 - \sum_{j=1}^{m_n} A_j e^{-s\tau_j})^{-1} B. \quad (30)$$

The operator  $\tilde{\Delta}$  is already defined in (25). The feedback interconnection (29) can represent the decentralised control system given by (2) and (16), affected by perturbations, represented by the signals  $f$  and  $g$ , at the state and with zero initial condition. Since  $\mathbf{G}$  is linear and time-invariant, the induced- $\mathcal{L}_2$  norm satisfies  $\|\mathbf{G}\|_{\mathcal{L}_2} = \|G\|_{\mathcal{H}_\infty}$ . We recall the small gain theorem that has been adapted from [15] for our problem setting as follows.

**Theorem 3.1.** *The mapping*

$$\begin{bmatrix} f \\ g \end{bmatrix} \longrightarrow \begin{bmatrix} w \\ z \end{bmatrix}, \quad (31)$$

*resulting from the feedback interconnection of (29) has a finite  $\mathcal{L}_2$  gain if  $\|G\|_{\mathcal{H}_\infty} \cdot \|\tilde{\Delta}\|_{\mathcal{L}_2} < 1$ .*

We consider a feedback interconnection of the form (29) to be input-output  $\mathcal{L}_2$  stable when its mapping (31) has a finite  $\mathcal{L}_2$  gain. Based on Assumption 1, we introduce the following lemma.

**Lemma 3.2.** *The integral operators  $\Delta_1^i, \Delta_2^i$ , and  $\Delta_3^i$  satisfy*

$$\|\Delta_j^i\|_{\mathcal{L}_2} \leq \gamma_j^i, \quad j = 1, 2, 3, \quad i = 1, \dots, N, \quad (32)$$

where

$$\begin{aligned} \gamma_1^i &= \bar{h}_i + \bar{\delta}_i, \\ \gamma_2^i &= \bar{\kappa}_i + \bar{\alpha}_i, \\ \gamma_3^i &= \bar{h}_i + \bar{\eta}_i, \quad i = 1, \dots, N. \end{aligned} \quad (33)$$

**Proof.** The proof is given in the appendix.  $\square$

To determine a condition for input-output stability of the feedback interconnection of (29), the following lemma is presented.

**Lemma 3.3.** *The  $\mathcal{L}_2$  gain of the operator  $\tilde{\Delta}_i$  can be bounded as follows,*

$$\|\tilde{\Delta}_i\|_{\mathcal{L}_2} \leq \bar{\gamma}_i, \quad (34)$$

where

$$\bar{\gamma}_i := \max\{\sqrt{(\gamma_1^i)^2 + (\gamma_3^i)^2}, \gamma_2^i\}, \quad i = 1, \dots, N. \quad (35)$$

**Proof.** The proof follows from Lemma 3.2 and by considering the worst-case  $\mathcal{L}_2$  gain.  $\square$

Combining the above results, a sufficient condition for input-output stability of the feedback interconnection of (29) is presented in the following theorem.

**Theorem 3.4.** *Assume that the nominal system described using the transfer function matrix defined in (30) is exponentially stable. Then, the feedback interconnection (29) (as in Figure 5) is guaranteed to be input-output  $\mathcal{L}_2$  stable if it satisfies the condition,*

$$\max_{i \in \{1, \dots, N\}} \bar{\gamma}_i < \left( \|G(j\omega)\|_{\mathcal{H}_\infty} \right)^{-1},$$

where the transfer function  $G(j\omega)$  from  $w$  to  $z$  is defined in (30) and  $\bar{\gamma}_i$  are defined in terms of the sampling interval and asynchrony bounds in (33) and (35).

**Proof.** The proof follows directly by virtue of Theorem 3.1 and Lemma 3.3.  $\square$

Next, we introduce a less conservative robust stability condition by exploiting the structure of the operator  $\tilde{\Delta}$ . To do so, we rely on scaling the feedback connection according to the structure of the block diagonal operator  $\tilde{\Delta}$  (see [33, 39] and the references therein for more details). We define (diagonal) scaling matrices  $X$  and  $\tilde{X}$ , such that

$$\begin{aligned} X &:= \begin{bmatrix} \check{\delta}_1 & \dots & 0 \\ \vdots & \ddots & \vdots \\ 0 & \dots & \check{\delta}_N \end{bmatrix}, \quad \tilde{X} := \begin{bmatrix} \hat{\delta}_1 & \dots & 0 \\ \vdots & \ddots & \vdots \\ 0 & \dots & \hat{\delta}_N \end{bmatrix}, \\ \check{\delta}_i &= \begin{bmatrix} \delta_{i,1} & 0 \\ 0 & \delta_{i,2} \end{bmatrix}, \quad \hat{\delta}_i = \begin{bmatrix} \delta_{i,1} I_{2 \times 2} & 0 \\ 0 & \delta_{i,2} \end{bmatrix}, \quad i = 1, \dots, N, \end{aligned} \quad (36)$$

and  $\delta_{i,j} \in \mathbb{R} \setminus \{0\}$ ,  $i = 1, \dots, N$ ,  $j = 1, 2$ , are scalar parameters. Notice that  $X$  and  $\tilde{X}$  have a structure related to



$\tilde{\Delta}$ , and  $\tilde{X} \neq X$  because the dimensions of input and output vectors are different. For simplicity of the presentation, we combine all the scalar parameters in a vector  $\tilde{\delta}$  where  $\tilde{\delta} = [\delta_{1,1} \ \delta_{1,2} \ \dots \ \delta_{N,1} \ \delta_{N,2}]^T$ . For the block-diagonal operator considered we have, by definition,  $X^{-1}\tilde{\Delta}\tilde{X} = \tilde{\Delta}$ . Due to the feedback interconnection of (27)-(28), we know that introducing the scaling matrices does not affect its stability property. We are now ready to improve the criterion from Theorem 3.4 using the following proposition.

**Proposition 3.5.** *Assume that the nominal system (30) is exponentially stable. Then, a sufficient condition for the feedback interconnection of (29) to be input-output  $\mathcal{L}_2$  stable is*

$$\max_{i \in \{1, \dots, N\}} \bar{\gamma}_i < \left( \inf_{\tilde{\delta}} \|X(\tilde{\delta})G(j\omega)\tilde{X}^{-1}(\tilde{\delta})\|_{\mathcal{H}_\infty} \right)^{-1}. \quad (37)$$

For simplicity of the presentation, we define a new (transfer) function  $\hat{G}(j\omega, \tilde{\delta}) := XG\tilde{X}^{-1}(j\omega, \tilde{\delta})$ .

**Remark 4.** *The values for the scaling parameters ( $\tilde{\delta}$ ) in (37) are determined by solving a non-convex optimisation problem. This problem will be shown later in Section 4.1.*

## 4. Controller design

We build on the approach of [9, 18, 32] to directly optimise the robustness against control imperfections (by minimising  $\|G\|_{\mathcal{H}_\infty}$ ) of the nominal time-delay system (24) as a function of the controller parameters. Notice that an exponentially stable nominal continuous-time system (24) is required to initialise the optimisation of objective functions involving the  $\mathcal{H}_\infty$  norm. If this is not the case, a preliminary stabilisation phase is conducted based on optimising the spectral abscissa. The spectral abscissa (stability) and  $\mathcal{H}_\infty$  norm (robustness) are, in general, non-smooth non-convex functions of fixed-order controller parameters [18, 32]. The work of [18, 32] generalises the one underlying the HIFOO package (see [5]) and the MATLAB function hinfstruct (see [1]) from finite-dimensional systems to that considering time-delay systems.

The vector  $\bar{p}$  contains the tunable parameters of the decentralised controllers

$$\bar{p}^T = [\bar{p}_1^T \ \dots \ \bar{p}_N^T], \text{ where } \bar{p}_i = \text{vec} \left( \begin{bmatrix} A_{ci} & B_{ci} \\ C_{ci} & D_{ci} \end{bmatrix} \right), \quad (38)$$

$i = 1, \dots, N$ . For the special case of static controller (as considered by [41]), only elements of  $D_{ci}$  exist. In the following subsections, we describe the objective functions for which the controller parameters may be optimised.

### 4.1. Generic case

The spectral abscissa of the nominal system (24) with  $w \equiv 0$  is defined as follows,

$$c(\bar{p}) = \sup_{\lambda \in \mathbb{C}} \{\Re(\lambda) : \det M(\lambda, \bar{p}) = 0\}, \quad (39)$$

where the characteristic matrix

$$M(\lambda, \bar{p}) := \lambda E - A_0(\bar{p}) - \sum_{i=1}^{m_n} A_i e^{-\lambda \tau_i}.$$

Note that the dependence of functions on  $\bar{p}$  is only made explicit in the notation when necessary. The exponential stability of the null solution of (24) is determined by the condition  $c(\bar{p}) < 0$  (see [32]). We know that the null solution of (24) is exponentially stable iff  $c(\bar{p}) < 0$ . With respect to the optimisation problem, the objective function is tuned with respect to the controller parameters ( $\bar{p}$ ). To obtain an exponentially stable system that maximises the exponential decay rate of the solutions, the controller parameters (in  $\bar{p}$ ) are optimised for the minimum of spectral abscissa, that is, they are obtained by

$$\min_{\bar{p}} c(\bar{p}). \quad (40)$$

The transfer function from  $w$  to  $z$  of the nominal system represented by (24) is given by

$$G(s, \bar{p}) = C \left( sE - A_0(\bar{p}) - \sum_{i=1}^{m_n} A_i e^{-s \tau_i} \right)^{-1} B. \quad (41)$$

Given that system (24) is exponentially stable, that is  $c(\bar{p}) < 0$ , the  $\mathcal{H}_\infty$  norm of the transfer function given in (41) can be expressed as

$$\|G(j\omega, \bar{p})\|_{\mathcal{H}_\infty} = \sup_{\omega \in \mathbb{R}} \sigma_1(G(j\omega, \bar{p})). \quad (42)$$

To improve robustness against control imperfections written in terms of the  $\mathcal{H}_\infty$  norm of (42), controller parameters (in  $\bar{p}$ ) may be optimised by minimising the function

$$\min_{\bar{p}} \|G(j\omega, \bar{p})\|_{\mathcal{H}_\infty}. \quad (43)$$

Thereby improving the maximum allowable upper-bound for the sampling intervals and asynchrony for which the closed-loop system is stable. The objective functions may be minimised using the algorithm in [9, 18], which uses the gradient-based optimisation algorithm HANSO [36] to handle the non-smooth optimisation problem.

For a less conservative result, it is also possible to consider Proposition 3.5 and simultaneously tune parameters in both  $\tilde{\delta}$  and  $\bar{p}$  to minimise

$$\min_{\tilde{\delta}, \bar{p}} \|\hat{G}(j\omega, \tilde{\delta}, \bar{p})\|_{\mathcal{H}_\infty}. \quad (44)$$

Alternatively, it is possible to consider a two layer (min-min) optimisation problem, wherein the outer layer tunes  $\bar{p}$  and inner layer tunes  $\tilde{\delta}$  for minimising the function

$$\min_{\bar{p}} \left( \min_{\tilde{\delta}} \|\hat{G}(j\omega, \tilde{\delta}, \bar{p})\|_{\mathcal{H}_\infty} \right). \quad (45)$$

Although optimisation problems (44) and (45) have the same solution, the numerical implementation may lead to different results. Since these optimisation problems are in general

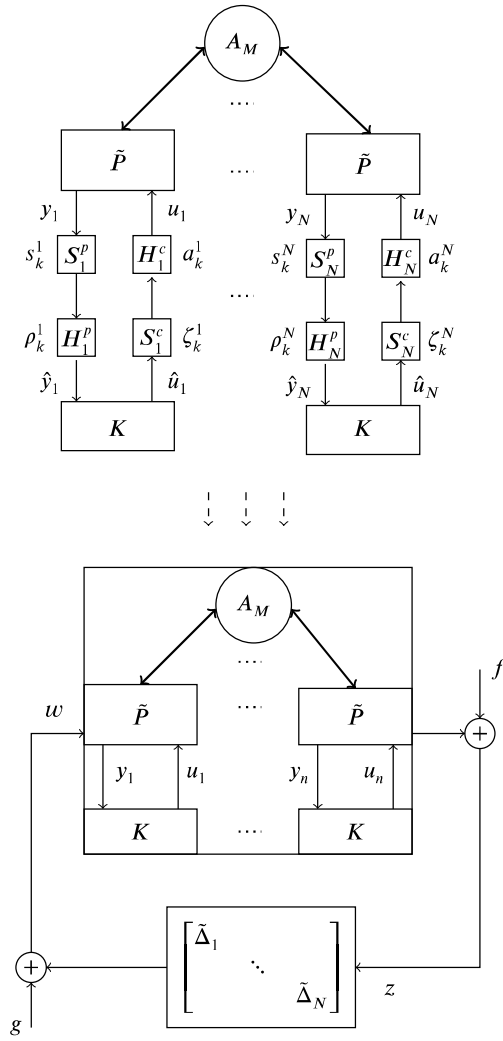


**Figure 6:** The structured MIMO system considered in this paper. Identical subsystems  $\tilde{P}$  (with constant time-delays at input, output, and state) connected through some network (described by the adjacency matrix  $A_M$ ) are to be stabilised by identical local (fixed-order) controllers with non-identical control imperfections.

non-convex, the local minima found may not correspond to each other. We use the gradient based optimisation algorithm HANSO to solve the optimisation problems of (44) and (45). We compute gradients for the optimisation problems using the approach in [18].

#### 4.2. Network structure exploitation

In this section, the special case of structured MIMO plant as in (5) is considered. Assume that the identical subsystems are to be controlled using identical fixed-order controllers, that is,  $A_{ci} = \bar{A}_c$ ,  $B_{ci} = \bar{B}_c$ ,  $C_{ci} = \bar{C}_c$ , and  $D_{ci} = \bar{D}_c \forall i = 1, \dots, N$  in (27), see Figure 6. Let us consider an augmented (sub-)system state vector  $x_i^T = [x_{pi}^T \ u_i^T \ \gamma_{wi}^T \ \gamma_{zi}^T \ x_{ci}^T \ y_i^T] \forall i = 1, \dots, N$ , where  $\gamma_{zi}$  and  $\gamma_{wi}$  are dummy vectors used to represent  $z_i$  and  $w_i$  respectively. Then, we can rewrite the closed-loop system of (5) and identical fixed-order controllers using

the state vector  $x^T = [x_1^T \ \dots \ x_n^T]$  as

$$\begin{cases} I \otimes \bar{E}_{cl} \dot{x}(t) = (I \otimes \bar{A}_{cl,0} + A_M \otimes \bar{F}_{cl})x(t) \\ \quad + \sum_{k=1}^{m_n} I \otimes \bar{A}_{cl,k} x(t - \tau_k) + I \otimes \bar{B}_{cl} w(t), \\ z(t) = I \otimes \bar{C}_{cl} x(t), \end{cases} \quad (46)$$

and at the level of uncertainty operator, there is no change from (25). The coefficient matrices in (46) are

$$\bar{A}_{cl,0} = \begin{bmatrix} \bar{A}_{p0} & \bar{B}_p & 0 & 0 & 0 & 0 \\ 0 & -I & [0 \ I \ \bar{D}_c] & 0 & \bar{C}_c & \bar{D}_c \\ 0 & 0 & -I & 0 & 0 & 0 \\ 0 & 0 & 0 & I & 0 & 0 \\ 0 & 0 & [\bar{B}_c \ 0 \ 0] & 0 & \bar{A}_c & \bar{B}_c \\ \bar{C}_p & 0 & 0 & 0 & 0 & -I \end{bmatrix},$$

$$\bar{A}_{cl,k} = \begin{bmatrix} \bar{A}_{pi} & 0 & 0 & 0 & 0 & 0 \\ 0 & 0 & 0 & 0 & 0 & 0 \\ 0 & 0 & 0 & 0 & 0 & 0 \\ 0 & 0 & 0 & 0 & 0 & 0 \\ 0 & 0 & 0 & 0 & 0 & 0 \\ 0 & 0 & 0 & 0 & 0 & 0 \end{bmatrix},$$

$$\bar{E}_{cl} = \begin{bmatrix} \bar{E}_p & 0 & 0 & 0 & 0 & 0 \\ 0 & 0 & 0 & 0 & 0 & 0 \\ 0 & 0 & 0 & 0 & 0 & 0 \\ [\bar{C}_p] & 0 & 0 & 0 & [0] & 0 \\ 0 & 0 & 0 & 0 & I & 0 \\ 0 & 0 & 0 & 0 & 0 & 0 \end{bmatrix},$$

$$\bar{F}_{cl} = \begin{bmatrix} \bar{F}_p & 0 & 0 & 0 & 0 & 0 \\ 0 & 0 & 0 & 0 & 0 & 0 \\ 0 & 0 & 0 & 0 & 0 & 0 \\ 0 & 0 & 0 & 0 & 0 & 0 \\ 0 & 0 & 0 & 0 & 0 & 0 \\ 0 & 0 & 0 & 0 & 0 & 0 \end{bmatrix}, \quad \bar{B}_{cl} = \begin{bmatrix} 0 \\ 0 \\ I \\ 0 \\ 0 \\ 0 \end{bmatrix},$$

$$\bar{C}_{cl} = [0 \ 0 \ 0 \ I \ 0 \ 0].$$

**Remark 5.** Plant (5) has no exogenous inputs or outputs; however, it is possible to consider other exogenous inputs or outputs (with identical coefficient matrices) in the nodal dynamics in addition to the control imperfections. Such a system can also be recast into the form of (46) with minor changes in the coefficient matrices, input vector, and output vector.

According to the complex Schur decomposition theorem [31], there always exists a unitary matrix  $T$  such that

$$A_M = T Z T^*, \quad (47)$$

where  $Z$  is an upper triangular matrix. Then, by performing a similarity transformation using  $\bar{x} = (T \otimes I)x$  and using the property that some matrices commute (like  $(T \otimes I)(I \otimes \bar{B}_{cl}) = (I \otimes \bar{B}_{cl})(T \otimes I)$ ) we obtain

$$z(t) = (T^* \otimes I)(I \otimes \bar{C}_{cl})\bar{x}(t). \quad (48)$$

It is clear from above that omitting the transformation by  $(T \otimes I)$  at input side and  $(T^* \otimes I)$  at output side in (48) does not affect the  $\mathcal{H}_\infty$  norm since  $T$  is unitary. In this paper, the control imperfections are considered only at the communication between controllers and plants. We recall the main result of authors in [9] which is summarised in the following theorem.

**Theorem 4.1.** *Let  $\{\lambda_{a1}, \dots, \lambda_{aN}\}$  denote the spectrum of  $A_M$ . Also, we consider the group of subsystems*

$$\begin{aligned} \bar{E}_{cl} \dot{\bar{x}}_i(t) &= (\bar{A}_{cl,0} + \lambda_{ai} \bar{F}_{cl}) \bar{x}_i(t) + \sum_{k=1}^{m_n} \bar{A}_{cl,k} \bar{x}_i(t - \tau_k) \\ &\quad + \bar{B}_{cl} \bar{w}_i(t), \\ \bar{z}_i(t) &= \bar{C}_{cl} \bar{x}_i(t), \quad i = 1, \dots, N. \end{aligned} \quad (49)$$

Then, the following results hold:

1. System (46) with  $w \equiv 0$  is exponentially stable if and only if the system (49) with  $\bar{w}_i \equiv 0$  for all  $i = 1, \dots, N$  is exponentially stable. Moreover the spectral abscissa  $c(\bar{p})$  of (46) satisfies

$$c(\bar{p}) = \max_{i \in \{1, \dots, N\}} \tilde{c}(\bar{p}, \lambda_{ai}), \quad (50)$$

where

$$\tilde{c}(\bar{p}, \lambda_{ai}) = \sup_{\lambda \in \mathbb{C}} \{\Re(\lambda) : \det \bar{M}(\lambda, \lambda_{ai}, \bar{p}) = 0\}, \quad (51)$$

and the characteristic matrix

$$\bar{M}(\lambda, \lambda_{ai}, \bar{p}) := \lambda \bar{E}_{cl} - \bar{A}_{cl,0}(\bar{p}) - \lambda_{ai} \bar{F}_{cl} - \sum_{k=1}^{m_n} \bar{A}_{cl,k} e^{-\lambda \tau_k}. \quad (52)$$

2. If  $A_M$  is a normal matrix, then

$$\|G(jw, \bar{p})\|_{\mathcal{H}_\infty} = \max_{i \in \{1, \dots, N\}} \|\tilde{G}(jw, \lambda_{ai}, \bar{p})\|_{\mathcal{H}_\infty}, \quad (53)$$

where  $\tilde{G}(jw, \lambda_{ai}, \bar{p})$  is the transfer functions of system (49) from  $\bar{w}_i$  to  $\bar{z}_i$ .

**Proof.** The assertions for the first part of Theorem 4.1 directly follow from the block-triangular structure of (48), with (49) appearing as the diagonal blocks, and from the structure of the associated eigenvalue problem. For the second part, recall that the Schur complex decomposition and spectral decomposition coincide for normal matrices. We refer to [9] for the extended version of the proof.  $\square$

**Corollary 4.2.** *Assume that  $A_M$  is normal. Then, a sufficient condition for the feedback interconnection of (29), for the case where system (24) is structured as in (46), to be input-output  $\mathcal{L}_2$  stable becomes*

$$\max_{i \in \{1, \dots, N\}} \bar{\gamma}_i < \left( \max_{i \in \{1, \dots, N\}} \|\tilde{G}(jw, \lambda_{ai}, \bar{p})\|_{\mathcal{H}_\infty} \right)^{-1}, \quad (54)$$

where

$$\tilde{G}(s, \lambda_{ai}, \bar{p}) = \bar{C}_{cl} \left( \bar{M}(s, \lambda_{ai}, \bar{p}) \right)^{-1} \bar{B}_{cl}.$$

**Proof.** The proof follows from Theorem 3.4 and the latter part of Theorem 4.1.  $\circ$

In order to design (more efficiently) identical decentralised controllers of the form (16) that are robust against control imperfections, we replace the minimisation objective (40) with

$$\min_{\bar{p}} \max_{i \in \{1, \dots, N\}} \tilde{c}(\bar{p}, \lambda_{ai}), \quad (55)$$

for faster exponential decay rate of the solutions and (43) with

$$\min_{\bar{p}} \max_{i \in \{1, \dots, N\}} \|\tilde{G}(jw, \lambda_{ai}, \bar{p})\|_{\mathcal{H}_\infty}, \quad (56)$$

for improving robustness against control imperfections. The network structure exploitation is performed by transforming the coupling between subsystems to some kind of *self-coupling* through  $\lambda_{ai}$ . The transformation matrices used to diagonalise the adjacency matrix must be unitary, which is satisfied when the adjacency matrix is a symmetric, corresponding to bi-directional coupling, or a circulant matrix.

The decoupling transformation based on Theorem 4.1, reduces the problem of a large system consisting of  $N$  subsystems to a parametrised subsystem (of lower dimension) [9]. Here, the parameters correspond to the eigenvalues of the adjacency matrix of the network graph through which the subsystems are connected. Recall that the dominant computational cost of evaluating the spectral abscissa and the  $\mathcal{H}_\infty$  norm amounts to computing the rightmost eigenvalues of a DDAE and the imaginary axis solutions of an associated Hamiltonian eigenvalue problem, respectively. In both cases the number of operations with the algorithms proposed in [18, 32] and the references therein scales with the cube of the dimension. That is, the computational complexity (or the number of operations with the algorithms) for optimising the spectral abscissa and  $\mathcal{H}_\infty$  norm of the overall system is reduced from the order of  $(N \cdot n_{cl})^3$  to  $N \cdot (n_{cl})^3$ . Notice that there is potential to arrive at scalable design methods whose cost does not depend on the number of subsystems (by handling the eigenvalue parameters as an uncertainty bounded in real interval using methods from robust control). This will be worked out in Section 5.

Notice that using the approach of network structure exploitation implies that we can no longer reduce conservatism using the scaling approach presented at the end of Section 3, since the scaling would not correspond to a unitary transformation.

## 5. Numerical example

In this section, we perform simulation-based studies on a numerical example made up of  $N$  identical third-order subsystems subject to different network and input perturbations. This example provides a simple illustration for the systems in Section 4.2. The simulations are performed using the MATLAB software tool described in [7], which relies on extending the results in [18, 32] towards scalable algorithms for the

design of sampled-data decentralised controllers. We specify the plant (5) as

$$\begin{cases} \dot{x}_{pi}(t) = \begin{bmatrix} -10 & 0 & 0 \\ 1 & 0 & 0 \\ 0 & 1 & 0 \end{bmatrix} x_{pi}(t) + \begin{bmatrix} 10 \\ 0 \\ 0 \end{bmatrix} u_i(t) + \Omega_i(t) \\ \quad + \sum_{j=1}^N a_{Mi,j} \begin{bmatrix} 1 & 0 & 0 \\ 0 & 1 & 0 \\ 0 & 0 & 0 \end{bmatrix} x_{pj}(t-0.2), \\ y_i(t) = \begin{bmatrix} 0 & 1 & 0 \\ 0 & 0 & 1 \end{bmatrix} x_{pi}(t-0.1), \quad i = 1, \dots, N, \end{cases} \quad (57)$$

where the normal adjacency matrix  $A_M$  has the elements

$$a_{Mi,j} = \begin{cases} 0.5, & \text{if } |i-j| = 1, \\ 0, & \text{otherwise,} \end{cases} \quad (58)$$

for all  $i, j = 1, \dots, N$ . In (57), there is an additional exogenous input vector  $\Omega_i(t)$  whose role will be discussed later on. The above plant is to be controlled by identical dynamic controllers of the form (9). The third and fourth equations of (corresponding) system (27) then take the form

$$\begin{cases} \dot{x}_{ci} = \bar{A}_c x_{ci} + \bar{B}_c y_i + \begin{bmatrix} \bar{B}_c & 0 & 0 \end{bmatrix} w_i(t), \\ u_i = \bar{C}_c x_{ci} + \bar{D}_c y_i + \begin{bmatrix} 0 & I & \bar{D}_c \end{bmatrix} w_i(t), \quad i = 1, \dots, N. \end{cases} \quad (59)$$

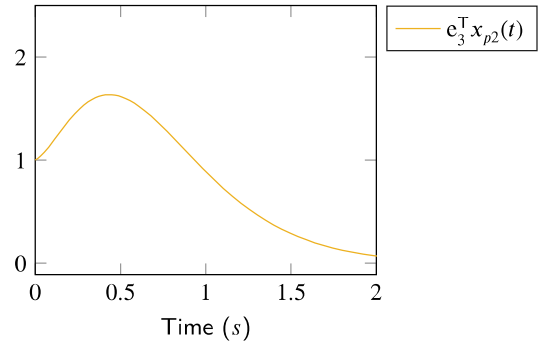
The exogenous outputs are

$$z_i(t) = \begin{bmatrix} C_g \dot{x}_{pi}(t) \\ \bar{C}_c \dot{x}_{ci}(t) \end{bmatrix}, \quad Y_i(t) = x_{pi}(t), \quad i = 1, \dots, N. \quad (60)$$

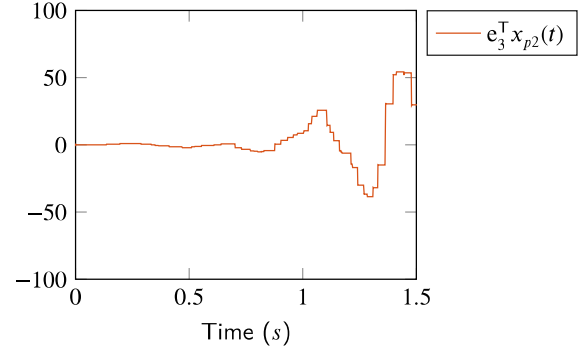
Notice that closed-loop system (57)-(60) is an example of the form (46) and hence we can exploit the network structure. However, we also consider new exogenous inputs ( $\Omega_i(t)$ ) to the subsystems in (57) and new exogenous outputs ( $Y_i(t)$ ) in (60). These terms allow us to consider some additional disturbances to the subsystems, besides the control imperfections. For example, these terms could provide an insight on the allowable parametric uncertainties on the plant's state-coefficient matrix. However, it can be easily shown that all the results presented in the previous sections still carry over to this situation.

First, we consider system (57)-(60) to be a small network with three subsystems ( $N = 3$ ). To illustrate the instability that may be caused due to the control imperfections in Figure 7, we use a second-order controller  $K_b$ , whose coefficient matrices are

$$\begin{aligned} \bar{A}_c &= 10^3 \cdot \begin{bmatrix} -2.4639 & -0.9459 \\ 2.796 & -2.2546 \end{bmatrix}, \\ \bar{B}_c &= 10^3 \cdot \begin{bmatrix} 0.0660 & -0.4056 \\ -0.2102 & 0.1232 \end{bmatrix}, \\ \bar{C}_c &= 10^3 \cdot \begin{bmatrix} 7.8543 & 1.0195 \end{bmatrix}, \\ \bar{D}_c &= 10^3 \cdot \begin{bmatrix} -0.2953 & 1.0865 \end{bmatrix}, \end{aligned} \quad (61)$$



(a) Continuous time system stabilised by the second-order controller  $K_b$  with no control imperfections. The spectral abscissa of the closed-loop system is -2.050.



(b) The closed-loop system is unstable when control imperfections are introduced.

**Figure 7:** Simulation of the closed-loop system (57) and  $K_b$ , when  $N = 3$ , for the initial value  $x_{pi}(0) = 1, x_{ci}(0) = 1 \forall i = 1, 2, 3$ . For clarity of presentation, we use only  $e_3^T x_{p2}$ , where  $e_3$  is the 3<sup>rd</sup> column vector of the identity matrix.

for each of the three subsystems in (57). The spectral abscissa of the closed-loop system of (57) and  $K_b$  is -2.050, when  $N = 3$ ,  $w_i \equiv 0$ ,  $\Omega_i \equiv 0$ ,  $i = 1, 2, 3$ . For the purpose of illustration, controller  $K_b$  was selected in such a way that the  $\mathcal{H}_\infty$  norm of the transfer function resulting from the corresponding closed-loop system was high.

We obtain a new controller  $K$  by minimising the  $\mathcal{H}_\infty$  norm of the transfer function of the system in (57)-(60), when  $N = 3$ , from

$$\hat{w} = [w_1^T \ w_2^T \ w_3^T \ \Omega_1^T \ \Omega_2^T \ \Omega_3^T]^T,$$

to

$$\hat{z} = [z_1^T \ z_2^T \ z_3^T \ Y_1^T \ Y_2^T \ Y_3^T]^T,$$

to 9.93 using the network structure exploiting algorithm. That is, a feedback interconnection of (57)-(60) and any bounded uncertainty operator with an induced- $\mathcal{L}_2$  norm less than  $\frac{1}{9.93}$  is input-output  $\mathcal{L}_2$  stable. For example, in addition to the control imperfections, closed-loop system (57)-(60), when  $N = 3$ , is also input-output  $\mathcal{L}_2$  stable for any (non-identical) perturbation on the subsystem's state ( $x_{pi}$ ) coefficient matrices which has an induced- $\mathcal{L}_2$  norm less than  $\frac{1}{9.93}$ .

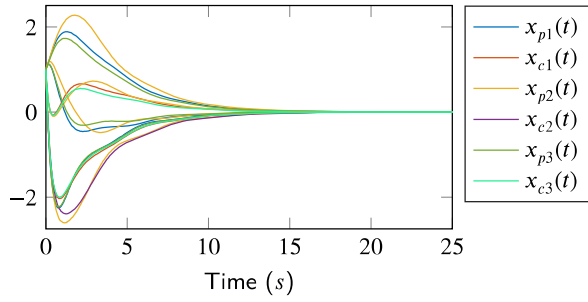


**Figure 8:** The closed-loop system of plant (57) and  $K$  with control imperfections, when  $N = 3$ , is stable even though it is slower than  $K_b$ . The spectral abscissa of plant (57) and  $K$  when  $\hat{w} \equiv 0$  is -0.3569. The upper-bounds for sampling intervals and asynchrony used in this simulation were defined to satisfy (54) (to verify the result presented in the previous section) and were identical to that used for the simulation of Figure 7b.

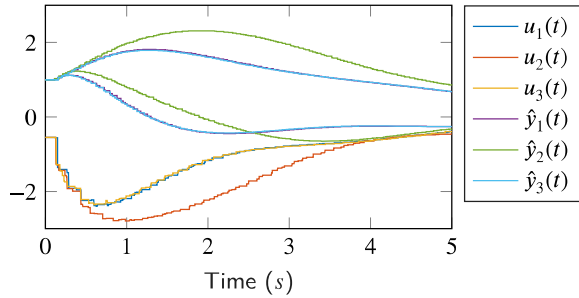


**Figure 9:** The input signals (received at plant) and output signals (received at controllers) corresponding to the plant (57) and  $K$  with control imperfections (using the settings same as Figure 8), when  $N = 3$ .

We observe that the  $\mathcal{H}_\infty$  norm corresponding to (only) control imperfections, when  $N = 3$ , from  $w = [w_1^T \ w_2^T \ w_3^T]^T$  to  $z = [z_1^T \ z_2^T \ z_3^T]^T$  while we assume  $\Omega_i \equiv 0$ ,  $i = 1, 2, 3$ , in (57)-(60) is equal to 5.81. The  $\mathcal{H}_\infty$  synthesis controller  $K$  has the coefficient matrices

$$\begin{aligned} \bar{A}_c &= \begin{bmatrix} -6.8101 & -0.0109 \\ -0.3745 & -4.5357 \end{bmatrix}, \quad \bar{B}_c = \begin{bmatrix} -2.9243 & 1.8633 \\ -4.0221 & -4.0900 \end{bmatrix}, \\ \bar{C}_c &= [0.0524 \quad 0.5468], \quad \bar{D}_c = [-0.6876 \quad -0.4615]. \end{aligned} \quad (62)$$

The simulation results for initial conditions of  $x_{pi}(t_0) = \bar{1}$ ,  $x_{ci}(t_0) = \bar{1}$ ,  $i = 1, 2, 3$ ,  $t_0 \leq 0$  are presented in Figures 8-9, where  $\bar{1}$  is used to represent a matrix or vector of appropriate dimension having all elements equal to 1. Note that the control imperfections (or the upper-bounds for the sampling intervals and asynchrony) were ensured to be the same ( $\frac{1}{5.8}$ ) for obtaining results using  $K_b$  in Figure 7 and using  $K$  in Figures 8-9 (see [7] for details on the software and numerical data used for the example).

Additionally, we note that the conservatism in these results was not negligible in simulations. Therefore, we aim at reducing the conservatism using the approach of Section 4.1.

**Table 1**

The  $\mathcal{H}_\infty$  norms computed for the closed-loop system of (57)-(60), when  $N > 3$ , from  $\hat{w}(= [w_1^T \ \dots \ w_N^T \ \Omega_1^T \ \dots \ \Omega_N^T]^T)$  to  $\hat{z}(= [z_1^T \ \dots \ z_N^T \ Y_1^T \ \dots \ Y_N^T]^T)$  with  $\bar{K}$  in (64) using the network structure exploitation approach.

$N$	$\mathcal{H}_\infty$ norm
10	11.8721
50	12.8393
100	12.8770
300	12.8885
500	12.8895

For this purpose, the scaling parameters ( $\delta_{i,j}$ ,  $i = 1, 2, 3$ ,  $j = 1, 2$  in (36)) are optimised using “1” (no scaling) as their initial value while not exploiting the network structure. Among other experiments, the “scaled”  $\mathcal{H}_\infty$  norm as in (45), when  $N = 3$ , from  $w$  to  $z$  was minimised (by tuning only  $\delta$ ) from 5.81 to 4.86 for the plant (57) and controller  $K$  in (62).

Suppose now that system (57)-(60) has a large number of subsystems ( $N \gg 3$ ), while retaining the same topology, then the general approach proposed in Section 4.1 becomes computationally cumbersome. The eigenvalues ( $\lambda_{ai}$ ) of  $A_M$  in (58) can be expressed as

$$\lambda_{ai} = \cos(i \frac{\pi}{N+1}), \quad i = 1, \dots, N, \quad (63)$$

that is,  $\lambda_{ai} \in [-1, 1] \ \forall i = 1, \dots, N$ . Therefore, an increase in the number of subsystems ( $N$ ) results in a denser distribution of the eigenvalues ( $\lambda_{ai}$ ) in the interval  $[-1, 1]$ . This allows us to extend the scalable algorithm for the design of stabilising controllers described in [6]. More precisely,  $\lambda_{ai}$  is interpreted as an uncertain parameter confined to the interval  $[-1, 1]$  and the worst case value of the  $\mathcal{H}_\infty$  norm is optimised over this interval (solving a min-max optimisation problem) to obtain a controller  $\bar{K}$  whose coefficient matrices are

$$\begin{aligned} \bar{A}_c &= \begin{bmatrix} -7.4310 & 0.9451 \\ -1.7851 & -6.9873 \end{bmatrix}, \quad \bar{B}_c = \begin{bmatrix} -3.5450 & 1.8700 \\ -2.2913 & -4.4404 \end{bmatrix}, \\ \bar{C}_c &= [-2.8900 \quad 1.5787], \quad \bar{D}_c = [-3.3538 \quad -0.0728]. \end{aligned} \quad (64)$$

$\bar{K}$  guarantees an upper bound on the  $\mathcal{H}_\infty$  norm (from  $\hat{w}$  to  $\hat{z}$ ) of 12.89, which is *independent* of the number of subsystems  $N$  in (57)-(60) and asymptotically exact as  $N \rightarrow \infty$  (see Table 1). Simulation based studies were also performed for the closed-loop system of (57)-(60), when  $N = 500$ , with  $\bar{K}$  in (64). Also, the sampling instants and delays were defined to satisfy the criterion in (54). The simulation results for the initial condition of  $x_{pi}(t_0) = \bar{1}$ ,  $x_{ci}(t_0) = \bar{1}$ ,  $i = 1, \dots, 500$ ,  $t_0 \leq 0$ , are presented in Figures 10-11. For simplicity of the presentation, simulation results of only three subsystems ( $i = 1, 250, 500$ ) are shown in Figures 10-11.



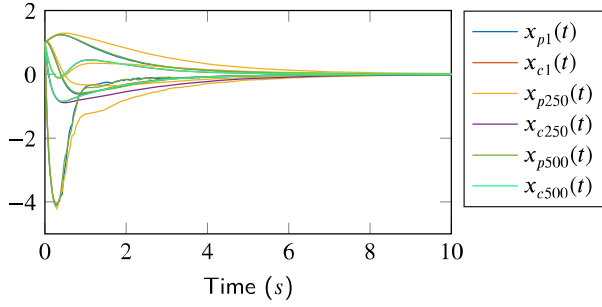


**Figure 10:** The closed-loop system of plant (57) and  $\bar{K}$  with control imperfections, when  $N = 500$ , is stable. The upper-bounds for sampling intervals and asynchrony used in this simulation were defined to satisfy (54) (to verify the result presented in the previous section).

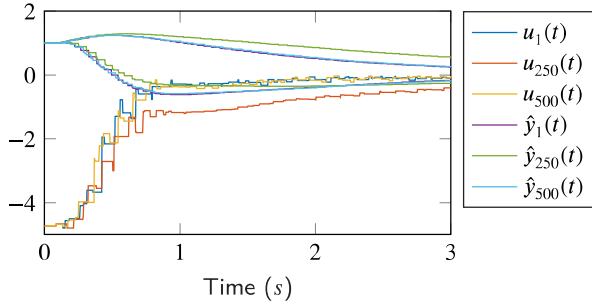


**Figure 11:** The input signals (received at plant) and output signals (received at controllers) corresponding to the plant (57) and  $\bar{K}$  with control imperfections (using the settings same as Figure 10), when  $N = 500$ .

## 6. Conclusion

In this paper, an approach to design stabilising decentralised controllers for generic MIMO plants which are robust against control imperfections (due to sampling and delays) and other input disturbances was proposed. The closed-loop system (with control imperfections) was rewritten as a feedback interconnection of a continuous-time closed-loop system and a bounded (integral) operator. The continuous-time closed-loop systems are modelled using DDAEs, which are flexible in modelling interconnected systems. Sparsity constraints are enforced in the parameterisation process within the optimisation to ensure that decentralised controllers are obtained.

The closed-loop system (with the sampled-data decentralised controllers) was rewritten as a feedback interconnection of a continuous-time closed-loop system and a bounded (integral) operator. This approach allowed us to use a simple input-output  $\mathcal{L}_2$  stability criterion based on the small gain theorem. Additionally, we proposed a method to reduce some conservativeness in the result, which exploits the structure of the operator. Furthermore, the computational efficiency of the controller design algorithm is significantly improved in the case of structured MIMO plant, wherein the plant is composed of quasi-identical subsystems, at the price

that the local controllers need to be identical and the scaling approach to reduce conservatism is not applicable anymore.

A frequency domain-based direct optimisation technique is proposed in this paper for controller design. Hence, issues related non-convexity and non-smoothness of the optimisation problem in general (especially for  $\mathcal{H}_\infty$  norm) are carried over from the centralised setting. We use the special algorithm HANSO to handle the non-smoothness. With respect to the non-convexity, the algorithm converges to local optima which may not global. This is mitigated by using sufficiently large number of randomly generated (or user specified) starting points for the optimisation problem.

## A. Upper-bound for the operators

In this section of Appendix, we present the preliminary lemmas required to prove Lemma 3.2 followed by the proof itself. First, we generalise the proof of Lemma 1 in [41]. For this purpose, we define new sequences  $\{b_l\}_{l \in \mathbb{Z}}$  where

$$b_{l+1} = b_l + \delta b_l, \quad l \in \mathbb{Z}, \quad (65)$$

$b_0 \in (0, \bar{\delta}b]$ , and  $\delta b_l \in (0, \bar{\delta}b]$ ,  $l \in \mathbb{Z}$ ,  $\bar{\delta}b \in \mathbb{R}^+$ . Also, the sequences  $\{c_l\}_{l \in \mathbb{Z}}$  satisfy

$$c_l = b_l + \delta c_l, \quad l \in \mathbb{Z}, \quad (66)$$

where  $\delta c_l \in [0, \bar{\delta}c] \forall l \in \mathbb{Z}$ ,  $\bar{\delta}c \in \mathbb{R}^+$ . Also, we define a *general* bounded integral operator  $\Delta$  on  $\mathcal{L}_{2e}(-\infty, \infty)$  that operates on the input based on the above sequences, that is

$$\begin{aligned} \hat{w}(t) &= (\Delta(\{b_l, c_l\}_{l \in \mathbb{Z}})\hat{z})(t) \\ &:= \int_{b_l}^t \hat{z}(\theta) d\theta, \quad \forall t \in [c_l, c_{l+1}), \quad l \in \mathbb{Z}. \end{aligned} \quad (67)$$

We abuse the notation for the operator as shown above, for  $\Delta(\{b_l, c_l\}_{l \in \mathbb{Z}})$ , to generalise it for any two sets of sequences that satisfy the above conditions as  $\{b_l\}_{l \in \mathbb{Z}}$  and  $\{c_l\}_{l \in \mathbb{Z}}$ . Now we prove the following lemma for this *general* operator.

**Lemma A.1.** *The operator  $\Delta(\{b_l, c_l\}_{l \in \mathbb{Z}})$  has an  $\mathcal{L}_2$  induced norm which is upper-bounded by  $\bar{\delta}b + \bar{\delta}c$ , that is,*

$$\|\Delta(\{b_l, c_l\}_{l \in \mathbb{Z}})\|_{\mathcal{L}_2} \leq \bar{\delta}b + \bar{\delta}c$$

**Proof.** By definition, we have

$$\hat{w}(t) = \int_{b_l}^t \hat{z}(\theta) d\theta, \quad \forall t \in [c_l, c_{l+1}), \quad l \in \mathbb{Z}. \quad (68)$$

Then by virtue of Jensen's inequality, we can write

$$\begin{aligned} \hat{w}(t)^T \hat{w}(t) &= \left( \int_{b_l}^t \hat{z}(\theta) d\theta \right)^T \left( \int_{b_l}^t \hat{z}(\theta) d\theta \right), \\ &\leq (t - b_l) \int_{b_l}^t \hat{z}^T(\theta) \hat{z}(\theta) d\theta, \quad \forall t \in [c_l, c_{l+1}), \\ &\leq (\bar{\delta}b + \bar{\delta}c) \int_{b_l}^t \hat{z}^T(\theta) \hat{z}(\theta) d\theta, \quad \forall t \in [c_l, c_{l+1}), \end{aligned}$$

(69)

since we know that  $t \in [c_l, c_{l+1})$

$$t - b_l \leq \overbrace{c_{l+1} - b_{l+1}}^{\leq \delta c} + \overbrace{b_{l+1} - b_l}^{\leq \delta b} \quad \forall t \in [c_l, c_{l+1}), \quad l \in \mathbb{Z}.$$

Substituting  $\theta = t + p$  in the above equation and using the fact  $t \in [c_l, c_{l+1})$ , we get

$$\hat{w}(t)^T \hat{w}(t) \leq (\delta b + \delta c) \int_{-(\delta b + \delta c)}^0 \hat{z}^T(t+p) \hat{z}(t+p) dp. \quad (70)$$

Integrating both the sides with respect to  $t$  in (70), we get

$$\begin{aligned} & \int_{-\infty}^{\infty} \hat{w}(t)^T \hat{w}(t) dt \\ & \leq (\delta b + \delta c) \int_{-\infty}^{\infty} \left( \int_{-(\delta b + \delta c)}^0 \hat{z}^T(t+p) \hat{z}(t+p) dp \right) dt, \quad (71) \\ & \leq (\delta b + \delta c) \int_{-(\delta b + \delta c)}^0 \left( \int_{-\infty}^{\infty} \hat{z}^T(t+p) \hat{z}(t+p) dt \right) dp, \end{aligned}$$

where  $\theta = t + p$ , since  $\theta \rightarrow \infty$  as  $t \rightarrow \infty$  and  $\theta \rightarrow -\infty$  as  $t \rightarrow -\infty$ , then we have

$$\begin{aligned} & \int_{-\infty}^{\infty} \hat{w}(t)^T \hat{w}(t) dt \\ & \leq (\delta b + \delta c) \int_{-(\delta b + \delta c)}^0 \left( \int_{-\infty}^{\infty} \hat{z}^T(\theta) \hat{z}(\theta) d\theta \right) dp. \quad (72) \end{aligned}$$

Consequently, we have

$$\|\hat{w}\|_{\mathcal{L}_2}^2 \leq (\delta b + \delta c)^2 \|\hat{z}\|_{\mathcal{L}_2}^2, \quad (73)$$

hence proved.  $\circ$

The idea underlying the proof of Lemma 3.2 is that the operators on  $\mathcal{L}_{2e}[0, \infty)$  considered in this paper can be seen as a special case of the operators on  $\mathcal{L}_{2e}(-\infty, \infty)$  considered by [41]. To illustrate this, we define the new sequences  $\{\hat{s}_l^i\}_{l \in \mathbb{Z}}$  in time to satisfy

$$\hat{s}_{l+1}^i = \hat{s}_l^i + \hat{h}_l^i, \quad l \in \mathbb{Z}, \quad i = 1, \dots, N, \quad (74)$$

where  $\hat{s}_k^i = s_k^i \quad \forall k \in \mathbb{Z}_0^+$ , and  $\hat{h}_l^i \in (0, \bar{h}_i] \quad \forall l \in \mathbb{Z}$ . Also, the sequences  $\{\hat{a}_l^i\}_{l \in \mathbb{Z}}$  satisfy

$$\hat{a}_l^i = \hat{s}_l^i + \hat{\eta}_l^i, \quad l \in \mathbb{Z}, \quad i = 1, \dots, N, \quad (75)$$

where  $\hat{a}_k^i = a_k^i \quad \forall k \in \mathbb{Z}_0^+$ ,  $\hat{\eta}_l^i \in [0, \bar{\eta}_i] \quad \forall l \in \mathbb{Z}$ , and  $\hat{a}_l^i < 0 \quad \forall l \in \mathbb{Z}^-$ . Using Lemma A.1, we know that

$$\|\Delta(\{\hat{s}_l^i, \hat{a}_l^i\}_{l \in \mathbb{Z}})\|_{\mathcal{L}_2} \leq \bar{h}_i + \bar{\eta}_i,$$

for any input (with finite energy) to the operator. We define two new operators, an extension operator  $\mathcal{D} : \mathcal{L}_{2e}[0, \infty) \rightarrow \mathcal{L}_{2e}(-\infty, \infty)$  such that

$$(\mathcal{D}\tilde{z})(t) := \begin{cases} \tilde{z}(t), & \forall t \in [0, \infty), \\ 0, & \forall t \in (-\infty, 0), \end{cases} \quad (76)$$

and a restriction operator  $\mathcal{R} : \mathcal{L}_{2e}(-\infty, \infty) \rightarrow \mathcal{L}_{2e}[0, \infty)$  such that  $\tilde{z}(t) = (\mathcal{R}\hat{z})(t) := \hat{z}(t) \quad \forall t \in [0, \infty)$ , then, we have the following lemma.

**Lemma A.2.** *The following relation holds true,*

$$(\Delta_3^i \tilde{z})(t) = (\mathcal{R}\Delta(\{\hat{s}_l^i, \hat{a}_l^i\}_{l \in \mathbb{Z}})\mathcal{D}\tilde{z})(t). \quad (77)$$

**Proof.** For the case when  $t \in [\hat{a}_{-1}^i, \hat{a}_0^i)$ , we know that  $\hat{a}_{-1}^i < 0 < \hat{a}_0^i$  then using (76) we have

$$\int_{\hat{s}_{-1}^i}^t \mathcal{D}\tilde{z}(\theta) d\theta = \begin{cases} \int_0^t \tilde{z}(\theta) d\theta, & \forall t \in [0, \hat{a}_0^i), \\ 0, & \forall t \in [\hat{a}_{-1}^i, 0), \end{cases} \quad (78)$$

Using the fact that  $\hat{a}_l^i < 0 \quad \forall l \in \mathbb{Z}^-$ , we also have

$$\begin{aligned} & (\Delta(\{\hat{s}_l^i, \hat{a}_l^i\}_{l \in \mathbb{Z}})\mathcal{D}\tilde{z})(t) \\ & = \begin{cases} \int_{\hat{s}_l^i}^t \mathcal{D}\tilde{z}(\theta) d\theta, & \forall t \in [\hat{a}_l^i, \hat{a}_{l+1}^i), \quad l \in \mathbb{Z}_0^+ \cup \{-1\}, \\ 0, & \forall t \in (-\infty, \hat{a}_{-1}^i). \end{cases} \quad (79) \end{aligned}$$

Then we can rewrite (79) using (78) as

$$\begin{aligned} & (\Delta(\{\hat{s}_l^i, \hat{a}_l^i\}_{l \in \mathbb{Z}})\mathcal{D}\tilde{z})(t) \\ & = \begin{cases} \int_{s_k^i}^t \tilde{z}(\theta) d\theta, & \forall t \in [a_k^i, a_{k+1}^i), \quad k \in \mathbb{Z}_0^+, \\ \int_0^t \tilde{z}(\theta) d\theta, & \forall t \in [0, a_0^i), \\ 0, & \forall t \in (-\infty, 0), \end{cases} \quad (80) \end{aligned}$$

hence proved.  $\circ$

**Proof of Lemma 3.2.** From Lemmas A.1 and A.2, we directly have

$$\|\Delta_3^i\|_{\mathcal{L}_2} \leq \|\Delta(\{\hat{s}_l^i, \hat{a}_l^i\}_{l \in \mathbb{Z}})\|_{\mathcal{L}_2} \leq \bar{h}_i + \bar{\eta}_i,$$

or  $\|\Delta_3^i\|_{\mathcal{L}_2} \leq \gamma_3^i$ ,  $i = 1, \dots, N$ . Similarly, using Lemma A.1 and slightly modifying Lemma A.2 (by changing the sequences in (74)-(75) accordingly), it can also be shown that  $\|\Delta_1^i\|_{\mathcal{L}_2} \leq \gamma_1^i$  and  $\|\Delta_2^i\|_{\mathcal{L}_2} \leq \gamma_2^i$ ,  $i = 1, \dots, N$ . Hence, Lemma 3.2 has been proved.  $\circ$

## References

- [1] Apkarian, P., Noll, D., 2006. Non-smooth H-infinity synthesis. IEEE Transactions on Automatic Control 51, 71–86.
- [2] Apkarian, P., Noll, D., 2018. Structured  $H_\infty$ -control of infinite-dimensional systems. International Journal of Robust and Nonlinear Control 28, 3212–3238.
- [3] Araujo, J., Mazo, M., Anta, A., Tabuada, P., Johansson, K.H., 2014. System architectures, protocols and algorithms for aperiodic wireless control systems. IEEE Transactions on Industrial Informatics 10, 175–184.
- [4] Bauer, N., Donkers, M., van de Wouw, N., Heemels, W., 2013. Decentralized observer-based control via networked communication. Automatica 49, 2074–2086.
- [5] Burke, J., Henrion, D., Lewis, A., Overton, M., 2006. HIFOO - a matlab package for fixed-order controller design and H-infinity optimization. IFAC Proceedings Volumes 39, 339–344. 5th IFAC Symposium on Robust Control Design.

- [6] Dileep, D., Borgioli, F., Hetel, L., Richard, J.P., Michiels, W., 2018a. A scalable design method for stabilising decentralised controllers for networks of delay-coupled systems, in: 5th IFAC Conference on Analysis and Control of Chaotic Systems, Netherlands.
- [7] Dileep, D., Michiels, W., 2019. tds\_hopt-nse-v2, a software tool for sampled data structured controller design for DDAEs with network structure exploitation. URL: [http://twr.cs.kuleuven.be/research/software/delay-control/tds\\_hopt-nse2.zip](http://twr.cs.kuleuven.be/research/software/delay-control/tds_hopt-nse2.zip).
- [8] Dileep, D., Michiels, W., Hetel, L., Richard, J.P., 2018b. Design of robust structurally constrained controllers for MIMO plants with time-delays, in: 2018 European Control Conference (ECC), pp. 1566–1571.
- [9] Dileep, D., Van Parys, R., Pipeleers, G., Hetel, L., Richard, J.P., Michiels, W., 2018c. Design of robust decentralised controllers for MIMO plants with delays through network structure exploitation. *International Journal of Control*.
- [10] Dolk, V., Borgers, D., Heemels, W., 2017. Output-based and decentralized dynamic event-triggered control with guaranteed  $\mathcal{L}_p$ -gain performance and zero-freeness. *IEEE Transactions on Automatic Control* 62, 34–49.
- [11] Donkers, M.C.F., Heemels, W.P.M.H., van de Wouw, N., Hetel, L., 2011. Stability analysis of networked control systems using a switched linear systems approach. *IEEE Transactions on Automatic Control* 56, 2101–2115.
- [12] Fiacchini, M., Morarescu, I., 2016. Stability analysis for systems with asynchronous sensors and actuators, in: 2016 IEEE 55th Conference on Decision and Control (CDC), pp. 3991–3996.
- [13] Fiter, C., Korabi, T.E., Etienne, L., Hetel, L., 2018. Stability of LTI Systems with Distributed Sensors and Aperiodic Sampling. Springer International Publishing. pp. 63–82.
- [14] Freris, N.M., Graham, S.R., Kumar, P.R., 2011. Fundamental limits on synchronizing clocks over networks. *IEEE Transactions on Automatic Control* 56, 1352–1364.
- [15] Fridman, E., 2014. Introduction to Time-Delay Systems: Analysis and Control. Systems & Control: Foundations & Applications, Springer International Publishing.
- [16] Fujioka, H., 2007. Stability analysis of systems with aperiodic sample-and-hold devices. *IFAC Proceedings Volumes* 40, 310 – 315. 7th IFAC Workshop on Time Delay Systems TDS 2007, Nantes, France, 1719 September, 2007.
- [17] Fujioka, H., Kao, C.Y., Almer, S., Jonsson, U., 2005. Sampled-data  $H_\infty$  control design for a class of pwm systems, in: Proceedings of the 44th IEEE Conference on Decision and Control.
- [18] Gumussoy, S., Michiels, W., 2011. Fixed-order  $H$ -infinity control for interconnected systems using delay differential algebraic equations. *SIAM Journal on Control and Optimization* 49, 2212–2238.
- [19] Heemels, W., Teel, A., van de Wouw, N., Nesic, D., 2010. Networked control systems with communication constraints: Tradeoffs between transmission intervals, delays and performance. *IEEE Transactions on Automatic Control* 55, 1781–1796.
- [20] Hetel, L., Fiter, C., Omran, H., Seuret, A., Fridman, E., Richard, J.P., Niculescu, S.I., 2017. Recent developments on the stability of systems with aperiodic sampling: An overview. *Automatica* 76, 309 – 335.
- [21] Hristu-Varsakelis, D., Levine, W., 2005. Handbook of Networked and Embedded Control Systems. Control Engineering - Birkhäuser, Birkhäuser Boston.
- [22] Jiang, X., Zhang, J., Harding, B.J., Makela, J.J., Domnguez-Garca, A.D., 2013. Spoofing gps receiver clock offset of phasor measurement units. *IEEE Transactions on Power Systems* 28, 3253–3262.
- [23] Kao, C., Cantoni, M., 2015. Robust performance analysis of aperiodic sampled-data feedback control systems, in: 2015 54th IEEE Conference on Decision and Control (CDC), pp. 1421–1426.
- [24] Kao, C.Y., Lincoln, B., 2004. Simple stability criteria for systems with time-varying delays. *Automatica* 40, 1429 – 1434.
- [25] Kao, C.Y., Rantzer, A., 2007. Stability analysis of systems with uncertain time-varying delays. *Automatica* 43, 959 – 970.
- [26] Lamnabhi-Lagarigue, F., Annaswamy, A., Engell, S., Isaksson, A., Khargonekar, P., Murray, R.M., Nijmeijer, H., Samad, T., Tilbury, D., den Hof, P.V., 2017. Systems and control for the future of humanity, research agenda: Current and future roles, impact and grand challenges. *Annual Reviews in Control* 43, 1 – 64.
- [27] Li, S.E., Zheng, Y., Li, K., Wu, Y., Hedrick, J.K., Gao, F., Zhang, H., 2017. Dynamical modeling and distributed control of connected and automated vehicles: Challenges and opportunities. *IEEE Intelligent Transportation Systems Magazine* 9, 46–58.
- [28] Lunze, J., 1992. Feedback control of large scale systems. Prentice-Hall international series in systems and control engineering, Prentice-Hall.
- [29] Manaffam, S., Talebi, M.K., Jain, A.K., Behal, A., 2017. Synchronization in networks of identical systems via pinning: Application to distributed secondary control of microgrids. *IEEE Transactions on Control Systems Technology* 25, 2227–2234.
- [30] McMillan, G.K., 2012. Industrial Applications of PID Control. Springer London, London.
- [31] Meyer, C., 2000. Matrix Analysis and Applied Linear Algebra: Other Titles in Applied Mathematics, Society for Industrial and Applied Mathematics.
- [32] Michiels, W., 2011. Spectrum-based stability analysis and stabilisation of systems described by delay differential algebraic equations. *IET Control Theory Applications* 5, 1829–1842.
- [33] Michiels, W., Fridman, E., Niculescu, S.I., 2009. Robustness assessment via stability radii in delay parameters. *International Journal of Robust and Nonlinear Control* 19, 1405–1426.
- [34] Mirkin, L., 2007. Some remarks on the use of time-varying delay to model sample-and-hold circuits. *IEEE Transactions on Automatic Control* 52, 1109–1112.
- [35] Naghshtabrizi, P., Hespanha, J.P., Teel, A.R., 2008. Exponential stability of impulsive systems with application to uncertain sampled-data systems. *Systems and Control Letters* 57, 378 – 385.
- [36] Overton, M.L., 2009. HANSO: a hybrid algorithm for non-smooth optimization. Computer Science, New York University.
- [37] Prieur, C., Queinnec, I., Tarbouriech, S., Zaccarian, L., 2018. Analysis and Synthesis of Reset Control Systems. now.
- [38] Samad, T., 2019. IFAC Industry Committee Update, Initiative to Increase Industrial Participation in the Control Community. Number 2 in Newsletters April 2019, IFAC.
- [39] Shamma, J.S., 1994. Robust stability with time-varying structured uncertainty. *IEEE Transactions on Automatic Control* 39, 714–724.
- [40] Siljak, D., 1991. Decentralized Control of Complex Systems. Mathematics in Science and Engineering, Elsevier Science.
- [41] Thomas, J., Hetel, L., Fiter, C., van de Wouw, N., Richard, J., 2018.  $\mathcal{L}_2$ -stability criterion for systems with decentralized asynchronous controllers, in: 2018 IEEE Conference on Decision and Control (CDC), pp. 6638–6643.
- [42] Toscano, R., 2013. Structured Controllers for Uncertain Systems: A Stochastic Optimization Approach. Advances in Industrial Control, Springer London.
- [43] Wakaiki, M., Okano, K., Hespanha, J.P., 2017. Stabilization of systems with asynchronous sensors and controllers. *Automatica* 81, 314 – 321.
- [44] Weitenberg, E., Jiang, Y., Zhao, C., Mallada, E., De Persis, C., Dörfler, F., 2019. Robust decentralized secondary frequency control in power systems: Merits and tradeoffs. *IEEE Transactions on Automatic Control* 64, 3967–3982.
- [45] Zegers, J.C., Semsar-Kazerooni, E., Ploeg, J., van de Wouw, N., Nijmeijer, H., 2018. Consensus control for vehicular platooning with velocity constraints. *IEEE Transactions on Control Systems Technology* 26, 1592–1605.
- [46] Zhang, W., Branicky, M.S., Phillips, S.M., 2001. Stability of networked control systems. *IEEE Control Systems Magazine* 21, 84–99.